Theor Chim Acta (1995) 90: 225–256

Theoretica
Chimica Acta

# Post-adiabatic approach to atomic and molecular processes: The van der Waals interactions of some open shell systems

**Vincenzo Aquilanti**[1], **Simonetta Cavalli**[1], **Lev Yu. Rusin**[2], **Mikhail B. Sevryuk**[2]
[1] Dipartimento di Chimica dell'Università, I-06100 Perugia, Italy
[2] Institute of Energy Problems of Chemical Physics, 117829 Moscow, Russia

Received February 15, 1994/Accepted June 9, 1994

**Summary.** Various properties of post-adiabatic representations of multichannel Schrödinger equations are described in the general context of adiabatic and classical path approximations as used in atomic and molecular physics. The van der Waals interactions of fluorine, chlorine, and oxygen atoms with rare gases, hydrogen, methane, and hydrogen halides are considered: it is found that in some of these systems, the first-order post-adiabatic scheme exhibits a smaller coupling than the adiabatic representation, thus providing an appropriate choice of the basis functions for a decoupling approximation.

**Key words:** Multichannel Schrödinger equation – Diabatic, adiabatic and post-adiabatic representations – Van der Waals interactions of O, F, Cl atoms

## 1. Introduction

In a recent paper [1] the properties of the adiabatic representation of a multichannel Schrödinger equation were analyzed by exploiting the Hamiltonian and symplectic nature of the coefficient and transformation matrices, respectively. Use of this algebraic structure of the problem was shown to be in line with an approach developed by Klar and Fano in their introduction of the post-adiabatic potentials (see Sect. 4). An infinite sequence of post-adiabatic representations was constructed and an algorithm for the choice of a symplectic transformation matrix for each representation was proposed. Those results, and in particular the recipes for obtaining the eigenvalues and eigenvectors of relevant manipulating matrices of half the size, were shown to offer interesting perspectives for the numerical integration of the multichannel Schrödinger equations, which arise when the solution of a quantum mechanical problem is tackled by the technique of separation of a variable.

In this paper we present various aspects of the post-adiabatic approach to atomic and molecular processes in the more general context of adiabatic and classical path Hamiltonians. Similarly to the usual diabatic and adiabatic representations, the post-adiabatic representations are based on the separation of all the degrees of freedom of the system in question into "fast" degrees of freedom and "slow" ones. The purely classical approach to atomic and molecular processes, i.e., a description of all the degrees of freedom (including electronic ones) within the framework of classical mechanics, is physically unsound since the motion of the electrons is essentially quantum mechanical. On the other hand, a quantum mechanical calculation of the features of a given process which treats all the degrees of freedom as enjoying equal rights cannot be practically performed even for very simple systems (at least by up-to-date computer equipment) and is physically unjustified due to the presence of a "small parameter", the ratio of the electron mass to the averaged mass of the nuclei. A tool to take adequately into account the difference in the masses of the electrons and nuclei is the celebrated Born–Oppenheimer procedure [2–4] of the separation of "slow" nuclear motions from "fast" electronic ones. Its prototypical character is here exploited for illustration purposes. This procedure leads to the concept of adiabatic potential energy surfaces. The motion of the nuclei can sometimes be considered as classical (the so-called classical path approximation in atomic and molecular physics [5]). On the other hand, after the "fast" degrees of freedom have been separated from the "slow" ones, the latter may be still described within the framework of quantum mechanics.

There are several options for such a description: (i) the (nonunique) *diabatic* representations [3, 6–8] connected with the quantum states of the reagents or products of the reaction or even of an intermediate coupling scheme; (ii) the *adiabatic* representation [3, 4, 8, 9], which takes into consideration the current configuration of the nuclei; and (iii) a hierarchy of *post-adiabatic* representations [1] (also taking into account the current configuration of the nuclei). In the construction of the post-adiabatic representations, the nonadiabatic coupling between the electronic states of the system is treated as a perturbation of the potential energy surfaces. This leads to new (post-adiabatic) potentials and a new (post-adiabatic) coupling which is sometimes *much smaller* than the initial coupling. The diabatic and adiabatic representations typically involve infinitely many equations, but only a finite number of them should be retained to proceed to the post-adiabatic representations.

Besides the classical path approximation, which treats the nuclear motions classically, an approximation of another kind is also widely exploited, namely, that of neglecting the nonadiabatic coupling between the potential energy surfaces. As a matter of fact, this approximation means that the process in question is assumed to evolve on a single potential energy surface and is described by the Schrödinger equation

$$i\hbar\frac{\partial\Psi(R,t)}{\partial t} = H_*(R)\Psi(R,t), \tag{1}$$

where $R$ are the coordinates of the nuclei, $\Psi(R, t)$ is the scalar wave function, while the Hamiltonian $H_*(R)$ has the form

$$H_*(R) = u(R) - \sum_\alpha \frac{\hbar^2}{2M_\alpha}\frac{\partial^2}{\partial R_\alpha^2}.$$

Here $u = u(R)$ is the potential energy surface under consideration and $M_\alpha$ are certain coefficients depending on the masses of the nuclei. As is well known, in the problem of a collision of two particles with masses $m_1$ and $m_2$ we have $M_1 = M_2 = M_3 = m_1m_2/(m_1 + m_2)$.

From the mathematical viewpoint, we have arrived at a problem of exactly the same form as the initial problem (before the separation of the electronic degrees of freedom):

$$i\hbar \frac{\partial \Psi(r, R, t)}{\partial t} = H(r, R)\Psi(r, R, t) \tag{2}$$

(here $r$ are the coordinates of the electrons). However, one can already perform quantum mechanical calculations in problem (1) treating all the degrees of freedom as enjoying equal rights. In many cases, a purely classical description of the nuclear motion in the field $u(R)$ is also justified (the method of classical trajectories [10, 11]). Finally, the nuclear degrees of freedom may also be partitioned into "fast" ones and "slow" ones depending on, e.g., the relative importance of the quantum effects. For example, in the problem of inelastic scattering of an atom by a diatomic molecule, it sometimes turns out to be useful to consider the translational and rotational degrees of freedom as "slow" ones and the vibrational degree of freedom of the molecule as a "fast" one [12]. After the separation of the "slow" motions from the "fast" ones the latter can be considered quantum mechanically whereas the "slow" motions may be described within the framework of classical mechanics (the classical path, or semiclassical, approximation for the nuclear degrees of freedom [12–15]). It is not expedient to treat the "slow" motions quantum mechanically if one has separated all the degrees of freedom into "fast" ones and "slow" ones just according to the relative strength of the quantum effects. Nevertheless, a quantum mechanical description of the "slow" motions may be useful in other cases.

It is here emphasized that the "slow" and "fast" degrees of freedom can be chosen as appropriate for a given problem and may bear no relation to electrons and nuclei (see, e.g., Ref. [9]); the most important example is the separation of the hyperradius in the hyperspherical approach to elementary processes (for our view see Ref. [16]).

The semiclassical theories based on the WKB approximation [5, 17] will not be dealt with in the present paper. We address the reader to our Ref. [18] for recent advances and references.

The structure of the paper is as follows. Section 2 recalls the derivation of the diabatic and adiabatic representations of multichannel Schrödinger equations while Sect. 3 describes, in a very brief way, the classical path approximation. The formal construction of the post-adiabatic representations is introduced in Sect. 4 and the basic properties of these representations are listed in Sect. 5. Section 6 treats in detail the simplest case of the construction, namely, the first-order post-adiabatic potentials and couplings in the two-state problem. The analysis of Sect. 6 is then applied in Sect. 7 to specific examples, the van der Waals interaction between O, F, Cl atoms and He, Ne, Ar, Kr, Xe, $D_2$, $CH_4$, HCl, HBr, HI particles. Several unsolved problems are mentioned in Sect. 8 by way of the conclusion. Finally, the Appendix is devoted to some important technical details of the post-adiabatic scheme which were not paid adequate attention in Ref. [1].

## 2 Adiabatic and diabatic representations and the nonadiabatic coupling operator

After the separation of the "slow" (or "external" [5]) coordinates $R$ from the "fast" (or "internal") ones $r$, independently of the physical motivation for the partition of all the degrees of freedom of the system into “fast” ones and “slow” ones, the Hamiltonian $H(r, R)$ of the problem takes the form

$$H(r, R) = H_0(r; R) - \sum_\alpha \frac{\hbar^2}{2M_\alpha} \frac{\partial^2}{\partial R_\alpha^2}, \tag{3}$$

where the “adiabatic” Hamiltonian $H_0 = H_0(r; R)$ involves no differentiation with respect to $R$. The eigenvalues $u_k(R)$ of the Hamiltonian $H_0$, which depend on the “slow” coordinates $R$ as on parameters, are called the *adiabatic potentials* (potential energy surfaces) of the problem in question.

Let $\varphi_k(r; R)$ be the corresponding orthonormalized eigenfunctions:

$$H_0\varphi_k = u_k\varphi_k, \quad \langle\varphi_k|\varphi_l\rangle = \delta_{kl} \tag{4}$$

(here $\delta_{kl}$ is the Kronecker symbol whereas the angle brackets denote integration over $r$). These functions also depend on the “slow” coordinates $R$ as on parameters. One can express the functions $\varphi_k$ in terms of an orthonormalized basis $\theta_k(r)$ independent of $R$:

$$\varphi_k(r; R) = \sum_l L_{lk}(R)\theta_l(r), \quad \langle\theta_k|\theta_l\rangle = \delta_{kl},$$

where the matrix elements $L_{lk} = L_{lk}(R)$ constitute a real orthogonal operator: $L^{t}L = I$, i.e.,

$$\sum_m L_{km}L_{lm} = \delta_{kl}.$$

Here and henceforth, the upper index t means a transposed (infinite) matrix, while $I$ denotes the identity operator. It is usually expedient to set $\theta_k(r) = \varphi_k(r; R^{(0)})$ where $R_\alpha^{(0)}$ are the values of the “slow” coordinates at the beginning or at the end of the system evolution. In particular, in the Born–Oppenheimer case, $\theta_k(r)$ can be taken as the quantum states of the reagents or products of the reaction.

One can look for the wave function $\Psi(r, R, t)$ of the system in the form

$$\Psi = \Psi(r, R, t) = \mathrm{e}^{-\mathrm{i}Et/\hbar}\sum_k \Theta_k(R)\theta_k(r), \tag{5}$$

where $E$ is the total energy of the system, or in the form

$$\Psi = \Psi(r, R, t) = \mathrm{e}^{-\mathrm{i}Et/\hbar}\sum_k \Phi_k(R)\varphi_k(r; R). \tag{6}$$

The coefficients $\Theta_k$ and $\Phi_k$ relate as

$$\Theta_k(R) = \sum_l L_{kl}(R)\Phi_l(R).$$

Substituting the expansions (5) and (6) into the Schrödinger equation (2), taking into account the special form (3) of the Hamiltonian $H(r, R)$, and recalling the definition (4) of the eigenfunctions $\varphi_k$, we arrive at the following equations for $\Theta_k$ or $\Phi_k$ (the so-called multichannel Schrödinger equations):

$$-\sum_\alpha \frac{\hbar^2}{2M_\alpha} \frac{\partial^2\Theta}{\partial R_\alpha^2} + V\Theta = E\Theta, \tag{7}$$

$$-\sum_\alpha \frac{\hbar^2}{2M_\alpha}\left(I\frac{\partial}{\partial R_\alpha} + P_\alpha\right)^2 \Phi + U\Phi = E\Phi. \tag{8}$$

In these equations, $U = U(R)$ is a diagonal operator (in the basis $\varphi_k$) with the diagonal elements $u_k$, the self-adjoint real potential energy operator $V = V(R)$ is equal to

$$V = LUL^t, \quad V_{kl} = \sum_m u_m L_{km} L_{lm},$$

and the skew-symmetric real operators $P_\alpha = P_\alpha(R)$ of the *nonadiabatic coupling* are equal to

$$P_\alpha = L^t \frac{\partial L}{\partial R_\alpha}, \quad P_{\alpha,kl} = \left\langle \varphi_k \left| \frac{\partial}{\partial R_\alpha} \right| \varphi_l \right\rangle. \tag{9}$$

Equation (7) is called the *diabatic representation* of the process under consideration, whereas Eq. (8) is called the *adiabatic representation* of this process. The diabatic representation, in contrast to the adiabatic one, shows no first derivatives with respect to the "slow" coordinates $R$ but involves the nondiagonal operator $V$ instead of the diagonal operator $U$. Moreover, the diabatic representation, again in contrast to the adiabatic one, is not unique [16], because the basis $\theta_k(r)$ can be *a priori* chosen in different ways and the operator $V(R)$ is defined only up to an $R$-independent orthogonal transformation of this basis.

One should emphasize that both representations – i.e., the diabatic (7) and adiabatic ones (8) – are exact. On the other hand, as we have already pointed out in Sect. 1, they typically consist of infinitely many equations, and the perspectives of their use in practical computations are determined by the rate of convergence of the corresponding finite-dimensional truncations.

Almost all the actual calculations for multichannel Schrödinger equations refer to the diabatic representation (7), an important early example being Ref. [19]. There are also some works dealing with the adiabatic representation (8); see Ref. [20] for pioneer examples and Ref. [21] for a recent survey. The possibilities for numerical integration of multichannel Schrödinger equations in the adiabatic representation are characterized by the behavior of the operators $P_\alpha$ of the nonadiabatic coupling (9). The smaller the $P_\alpha$ (i.e., the smaller an error with which the process under consideration can be represented as a collection of noninteracting single channel ones), the higher the calculation rate and accuracy for numerical solutions of Eq. (8). Moreover, the partition itself of all the coordinates in the configuration space into "fast" ones and "slow" ones is justified only when the matrix elements $P_{\alpha,kl}$ are small everywhere except for some localized regions. A quantitative measure of the coupling between two channels corresponding to the adiabatic potentials $u_k(R)$ and $u_l(R)$ is the dimensionless function

$$\frac{1}{|u_k(R) - u_l(R)|} \sum_\alpha \frac{\hbar^2}{2M_\alpha} |P_{\alpha,kl}(R)|^2. \tag{10}$$

The point of the maximum for function (10) coincides approximately with the location of the minimum for the term splitting $|u_k(R) - u_l(R)|$ (the so-called avoided crossing point [5]). In the classical path approach to a given process, the probability of the nonadiabatic transitions between the potential energy surfaces $u_k(R)$ and $u_l(R)$ attains a maximum in a vicinity of this point.

## 3 Classical path approach

Let us consider the classical path formalism in more detail. In order to describe the evolution of the "slow" coordinates $R$ within the framework of classical mechanics, we introduce the concept of a trajectory $R(t)$, the full Schrödinger equation (2) having to be replaced by the equation

$$i\hbar \frac{\partial \Psi_0(r, t)}{\partial t} = H_0(r; R(t))\Psi_0(r, t) \tag{11}$$

(recall that $H_0$ is the adiabatic Hamiltonian). Expanding the "fast" wave function $\Psi_0(r, t)$ in the adiabatic basis $\varphi_k(r; R)$,

$$\Psi_0 = \Psi_0(r, t) = \sum_k A_k(t)\varphi_k(r; R(t)),$$

and recalling the definition (4) of the eigenfunctions $\varphi_k$, we obtain the following equation for the coefficients $A_k$:

$$\frac{dA}{dt} = -\left(\frac{i}{\hbar} U + \sum_\alpha \frac{dR_\alpha}{dt} P_\alpha\right) A, \tag{12}$$

where $U = U[R(t)]$ and $P_\alpha = P_\alpha[R(t)]$. Here we have used the fact that

$$\left\langle \varphi_k \left| \frac{\partial}{\partial t} \right| \varphi_l \right\rangle = \sum_\alpha \frac{dR_\alpha}{dt} P_{\alpha,kl}$$

according to Eq. (9).

Analogously to the expansions (5) and (6), the functions $A_k$ are often represented in the form

$$A_k(t) = a_k(t) \exp\left\{ -\frac{i}{\hbar} \int_{t_0}^{t} u_k[R(\tau)]\, d\tau \right\},$$

the coefficients $a_k$ satisfying the equation

$$\frac{da}{dt} = -\sum_\alpha \frac{dR_\alpha}{dt} Q_\alpha a \tag{13}$$

where

$$Q_{\alpha,kl}(t) = P_{\alpha,kl}[R(t)] \exp\left\{ \frac{i}{\hbar} \int_{t_0}^{t} (u_k[R(\tau)] - u_l[R(\tau)])\, d\tau \right\}.$$

The probability of the transition $k \to l$ is equal to $|a_l(+\infty)|^2$ where $\{a_m(t)\}_m$ denotes the solution of Eq. (13) with the initial conditions $a_m(-\infty) = \delta_{mk}$.

Using the Ehrenfest average [12] of the Hamiltonian $H_0$

$$H_0^{\text{aver}}(R, t) = \langle \Psi_0 | H_0 | \Psi_0 \rangle = \sum_k |A_k(t)|^2 u_k(R) = \sum_k |a_k(t)|^2 u_k(R),$$

we arrive at the equations for the functions $R_\alpha(t)$:

$$M_\alpha \frac{d^2 R_\alpha}{dt^2} = -\frac{\partial H_0^{\text{aver}}}{\partial R_\alpha} = -\sum_k |A_k|^2 \frac{\partial u_k}{\partial R_\alpha} = -\sum_k |a_k|^2 \frac{\partial u_k}{\partial R_\alpha}. \tag{14}$$

One has to solve Eqs. (12), (14) [or (13), (14)] simultaneously determining the classical trajectories $R_\alpha(t)$ and the quantum mechanical amplitudes $a_k(t)$. There also exist other approaches to the derivation of the equations for the functions $R_\alpha(t)$ [5].

The smaller the $P_\alpha$, the higher the accuracy with which the system of Eqs. (13), (14) with the initial conditions $a_m(-\infty) = \delta_{mk}$ for some $k$ can be approximated by the system

$$a_m \equiv \delta_{mk}, \quad M_\alpha \frac{\mathrm{d}^2 R_\alpha}{\mathrm{d}t^2} = -\frac{\partial u_k}{\partial R_\alpha}$$

corresponding to the classical motion in the field $u_k$ in the absence of the other potential energy surfaces.

## 4 Hierarchy of the post-adiabatic representations

The crucial condition for effectively calculating a given multichannel process as a perturbation of a collection of noninteracting single channel processes is the smallness of the matrix elements $P_{\alpha,kl}$ given by Eq. (9). This condition is equally important for both the purely quantum mechanical approach to the process via the adiabatic representation (8) and the classical path approximation (12)–(13). In this context, the so-called *post-adiabatic representations* of an elementary chemical process introduced by Klar and Fano in 1976–1978 [22–24] are of considerable interest. These representations have the form similar to Eq. (8) but involve a new coupling which is sometimes *much smaller* than the initial nonadiabatic coupling. The Klar–Fano theory has been further developed and given a rigorous mathematical background in Ref. [1].

The post-adiabatic analysis can be applied only to problems containing a single "slow" coordinate $R$. The main idea of Klar and Fano is to "include", via certain algebraic operations, the nonadiabatic coupling in the potential curves $u_k(R) = u_k^{(0)}(R)$ for each value of $R$. This would result in new (post-adiabatic) potentials $u_k^{(1)}(R)$ and a new coupling $\Pi_1 = \Pi_1(R)$ which can be smaller than the initial coupling. One may then "include" this *residual* (post-adiabatic) coupling $\Pi_1$ in the post-adiabatic potentials $u_k^{(1)}(R)$ (again using algebraic operations only) and obtain the post-adiabatic potentials $u_k^{(2)}(R)$ of the second order and a coupling $\Pi_2 = \Pi_2(R)$. From the formal viewpoint, this iterative procedure (to be called the Klar–Fano construction in the sequel) consists of infinitely many steps, but it seems that the first step only is of practical significance. The reason is that neither conditions guaranteeing the decrease of the coupling at each step, nor convergence criteria for the iterations, nor properties of the limiting equation in the convergence case are known.

Up to now, the Klar–Fano construction has been developed only for systems with a finite number ($N$) of states $\varphi_k$. As the mathematical apparatus, the theory of Hamiltonian and symplectic matrices is exploited. Recall that a $2N \times 2N$ matrix $K$ is said to be Hamiltonian if it satisfies the condition $K^{\mathrm{t}}J + JK = 0$ where

$$J = \begin{pmatrix} 0 & -I \\ I & 0 \end{pmatrix}$$

and $I$ denotes the identity $N \times N$ matrix. A matrix $K$ is Hamiltonian if and only if it has the form

$$K = \begin{pmatrix} A & B \\ C & -A^{\mathrm{t}} \end{pmatrix}$$

where the $N \times N$ matrices $B$ and $C$ are symmetric: $B^t = B$, $C^t = C$ while the $N \times N$ matrix $A$ is arbitrary. Hamiltonian matrices determine Hamiltonian linear differential equations. On the other hand, a $2N \times 2N$ matrix $S$ is said to be symplectic if it satisfies the condition $S^t J S = J$. Symplectic matrices determine canonical linear transformations. A list of the basic properties of Hamiltonian and symplectic linear operators and a detailed description of the iterative procedure are presented in Ref. [1]. Here we will give just a brief summary of the algebraic operations at each iteration step. For other applications of Hamiltonian equations and canonical transformations to multichannel processes see, e.g., Ref. [25].

The starting point of the Klar–Fano construction is the adiabatic representation (8) where the number of the "slow" coordinates $R_\alpha$ is equal to 1 (so that the index $\alpha$ becomes unnecessary), $U(R)$ is a diagonal $N \times N$ matrix, $P(R)$ is a skew-symmetric $N \times N$ matrix, and $\Phi(R)$ denotes an $N$-dimensional vector. One can rewrite the system of $N$ second-order equations

$$-\frac{\hbar^2}{2M}\left(I\frac{\mathrm{d}}{\mathrm{d}R} + P\right)^2 \Phi + U\Phi = E\Phi$$

as a system of $2N$ first-order equations

$$\frac{\hbar}{\sqrt{2M}}\frac{\mathrm{d}}{\mathrm{d}R}\begin{pmatrix}\Phi\\ \Xi\end{pmatrix} + \left[\begin{pmatrix}0 & I\\ U - EI & 0\end{pmatrix} + \frac{\hbar}{\sqrt{2M}}\begin{pmatrix}P & 0\\ 0 & P\end{pmatrix}\right]\begin{pmatrix}\Phi\\ \Xi\end{pmatrix} = 0, \tag{15}$$

where

$$\Xi = -\frac{\hbar}{\sqrt{2M}}\left(I\frac{\mathrm{d}}{\mathrm{d}R} + P\right)\Phi.$$

The matrix

$$\Pi_0 = \begin{pmatrix}P & 0\\ 0 & P\end{pmatrix} \tag{16}$$

is Hamiltonian since $P$ is skew-symmetric whereas the matrix $U = U_0$ is diagonal with the diagonal elements $u_k^{(0)}$ which are the adiabatic potentials of the system in question.

In general, just before the $(s+1)$th iteration step ($s \geqslant 0$), we have a collection of $2N$ first-order equations

$$\frac{\hbar}{\sqrt{2M}}\frac{\mathrm{d}X}{\mathrm{d}R} + \left[\begin{pmatrix}0 & I\\ U_s - EI & 0\end{pmatrix} + \frac{\hbar}{\sqrt{2M}}\Pi_s\right]X = 0, \tag{17}$$

where $U_s = U_s(R)$ is a diagonal $N \times N$ matrix with the diagonal elements $u_k^{(s)}(R)$ (the *post-adiabatic potentials* of the system in question of order $s$ corresponding to the total energy $E$), $\Pi_s = \Pi_s(R)$ is a Hamiltonian $2N \times 2N$ matrix (the *post-adiabatic coupling* of order $s$ corresponding to the total energy $E$), and $X(R)$ denotes a $2N$-dimensional vector. The eigenvalues of the matrix

$$\begin{pmatrix}0 & I\\ U_s - EI & 0\end{pmatrix}$$

are equal to $\pm [u_k^{(s)} - E]^{1/2}$. Denote the eigenvalues of the Hamiltonian matrix

$$K_s = K_s(R) = \begin{pmatrix} 0 & I \\ U_s - EI & 0 \end{pmatrix} + \frac{\hbar}{\sqrt{2M}} \Pi_s \tag{18}$$

by $\pm [u_k^{(s+1)} - E]^{1/2}$ (recall that the spectrum of any Hamiltonian matrix consists of pairs $\pm \lambda$ [1]). The functions $u_k^{(s+1)}(R)$ are the post-adiabatic potentials of the given system of order $s + 1$ corresponding to the total energy $E$.

Suppose that for $R$ ranging in a certain interval the quantities $u_1^{(s+1)}, \dots, u_N^{(s+1)}$ are distinct and other than $E$. Let $U_{s+1} = U_{s+1}(R)$ be the diagonal matrix with the diagonal elements $u_k^{(s+1)}$. The Hamiltonian matrices $K_s$ and

$$\begin{pmatrix} 0 & I \\ U_{s+1} - EI & 0 \end{pmatrix} \tag{19}$$

possess the same simple spectrum and are therefore conjugated, at least over $C$, by a symplectic $2N \times 2N$ matrix $S_s = S_s(R)$ [1]:

$$S_s^{-1} K_s S_s = \begin{pmatrix} 0 & I \\ U_{s+1} - EI & 0 \end{pmatrix}.$$

Then the coordinate transformation

$$X = S_s Y$$

$[Y(R)$ being a $2N$-dimensional vector$]$ casts Eq. (17) into the equation

$$\frac{\hbar}{\sqrt{2M}} \frac{\mathrm{d}Y}{\mathrm{d}R} + \left[ \begin{pmatrix} 0 & I \\ U_{s+1} - EI & 0 \end{pmatrix} + \frac{\hbar}{\sqrt{2M}} \Pi_{s+1} \right] Y = 0, \tag{20}$$

where

$$\Pi_{s+1} = \Pi_{s+1}(R) = S_s^{-1} \frac{\mathrm{d}S_s}{\mathrm{d}R} \tag{21}$$

is a Hamiltonian $2N \times 2N$ matrix representing the post-adiabatic coupling of order $s + 1$ corresponding to the total energy $E$. Equation (20) is of the same form as Eq. (17) but involves $U_{s+1}$ and $\Pi_{s+1}$ instead of $U_s$ and $\Pi_s$, respectively, and is the starting point for the $(s + 2)$th iteration step.

In particular, the first-order post-adiabatic potentials $u_1^{(1)}, \dots, u_N^{(1)}$ corresponding to the total energy $E$ are equal, respectively, to $\lambda_1^2 + E, \dots, \lambda_N^2 + E$ where $\pm \lambda_1, \dots, \pm \lambda_N$ are the eigenvalues of the Hamiltonian matrix

$$K_0 = \begin{pmatrix} 0 & I \\ U - EI & 0 \end{pmatrix} + \frac{\hbar}{\sqrt{2M}} \begin{pmatrix} P & 0 \\ 0 & P \end{pmatrix} \tag{22}$$

(recall that $U$ is the diagonal matrix whose diagonal elements are the usual adiabatic potentials $u_1, \dots, u_N$, while $P$ is the skew-symmetric matrix of the nonadiabatic coupling). Let $U_1$ be the diagonal matrix whose diagonal elements are $u_1^{(1)}, \dots, u_N^{(1)}$ and $S_0$, a symplectic matrix satisfying the condition

$$K_0 S_0 = S_0 \begin{pmatrix} 0 & I \\ U_1 - EI & 0 \end{pmatrix}.$$

Then the matrix $\Pi_1$ of the first-order post-adiabatic coupling corresponding to the total energy $E$ is equal to

$$\Pi_1 = S_0^{-1} \frac{dS_0}{dR}.$$

The degeneracy (multiplicity) of the spectrum of matrix $K_s$ [Eq. (18)] can be an obstacle for this construction. Among the degeneracy points, one should distinguish the turning points $u_m^{(s+1)}(R) = E$ and the coalescence points $u_m^{(s+1)}(R) = u_n^{(s+1)}(R)$. At all these points, the coupling $\Pi_{s+1}$ and the subsequent post-adiabatic potentials $u_k^{(v)}$ and couplings $\Pi_v$, $v \geqslant s + 2$, are *a priori* not defined. However, as we will see in the Appendix, the turning points are in fact not dangerous for the post-adiabatic scheme.

If the coupling $\Pi_s$ is small then the turning and coalescence points for the potentials $u_k^{(s+1)}$ are close, respectively, to the turning and coalescence points for the potentials $u_k^{(s)}$.

What is of great importance for practical calculations is that finding the potentials $u_k^{(s+1)} = \lambda_k^2 + E$ ($\pm\lambda_k$ being the eigenvalues of the matrix $K_s$ of order $2N$) and constructing a symplectic operator $S_s$ conjugating two matrices (18) and (19) of order $2N$ can be reduced to manipulations of matrices of order $N$. The relevant methods are described in detail and given a rigorous proof in Ref. [1] and will not be reproduced here.

## 5 Peculiarities of the post-adiabatic scheme

As we will see in Sect. 7 by an example of the interaction of fluorine and chlorine atoms with rare gases, hydrogen, methane, and hydrogen halides, the post-adiabatic coupling $\Pi_1$ often turns out to be much smaller than the usual nonadiabatic coupling $P$. On the other hand, it is also necessary to mention some limitations of the post-adiabatic approach (however, not all of them are essential for practical computations).

### *The choice of the slow coordinate*

One can construct the post-adiabatic representations only for systems with a single "slow" coordinate. This circumstance may seem to be very restrictive, but for many applications, it is quite sufficient to consider such systems only. For instance, if the transitions between the terms of a given diatomic system are induced mainly by the radial relative motion of the atoms then one can neglect the rotation of the molecular axis while studying these transitions and take into account the internuclear distance as the only "slow" coordinate [26] (the "fast" variables are the electronic coordinates). This is just the case for the interactions O, F, Cl–He, Ne, Ar, Kr, Xe, $D_2$, $CH_4$, HCl, HBr, HI considered in Sect. 7.

Another example comes from the hyperspherical coordinates technique [14, 15, 25, 27–29]. A system of $n \geqslant 3$ atoms can be described by the hyperradius $\rho$ (a coordinate whose dimension is length) and $3n - 4$ angular variables [25, 27]. For example, for $n = 3$, the three coordinates ($\rho$, $\theta$, $\phi$) determine the internal configuration of a system of atoms A, B, C (i.e., the size and shape of the ABC triangle) whereas the three Euler angles ($\alpha$, $\beta$, $\gamma$) describe how the ABC triangle is oriented in space [14, 15, 28]. Within the semiclassical approach on a single potential energy surface, the internal coordinates are sometimes quantized whereas the Euler angles are treated classically [15]. On the other hand, it is also possible not to quantize the hyperradius [14] and, moreover, consider it as the only "slow" (and quasiseparable) variable [16, 25, 27] which enables one to apply the post-adiabatic scheme.

An opposite example is the semiclassical $V_qR_cT_c$ description of inelastic scattering of an atom by a diatomic molecule on a single potential energy surface, when the translational and rotational degrees of freedom are treated classically and the vibrational degree of freedom of the molecule is quantized [12]. Here we have five "slow" coordinates and one "fast" coordinate.

Fano, H. Klar, and M. Klar [22–24] considered scattering of an electron by a hydrogen atom and used the mean-square radius of the two electrons introduced by Fock [30] as the "slow" coordinate.

## *Nonuniqueness of the representation*

What is much more important is that the post-adiabatic representations are not determined uniquely. At each step of the Klar–Fano construction, one computes an $R$-dependent symplectic matrix $S_s$ conjugating the Hamiltonian matrices (18) and (19), and all the symplectic matrices conjugating two given Hamiltonian $2N \times 2N$ matrices with the same simple spectrum constitute an $N$-dimensional manifold. The post-adiabatic coupling $\Pi_{s+1}(R)$ of order $s+1$ and the post-adiabatic potentials $u_k^{(s+2)}(R)$ of order $s+2$ depend therefore upon the choice of the matrix-valued function $S_s(R)$ at the $(s+1)$th step of the iterative scheme.

In particular, whereas the first-order post-adiabatic potentials $u_k^{(1)}$ are determined uniquely by the system itself (as well as the usual adiabatic potentials $u_k$ and nonadiabatic coupling $P$), the first-order post-adiabatic coupling $\Pi_1$ already depends upon the choice of $S_0$.

The problem of the optimal choice of the function $S_s(R)$ at each iteration step therefore arises when using the post-adiabatic representations of the process in question. One can call *optimal* the function $S_s(R)$ which minimizes the coupling $\Pi_{s+1}(R)$. An unsuitable choice of $S_s$ may result in a very large post-adiabatic coupling of order $s+1$. In a general setup, the problem of the choice of the matrix $S_s$ seems to be very hard (not to mention the fact that the magnitude of the coupling $\Pi_{s+1}$ can also be defined in several different ways). In Ref. [1], we have proposed a rather simple and effective algorithm for the choice of the matrix $S_s$ which guarantees a small coupling $\Pi_{s+1}(R)$ provided that the coupling $\Pi_s(R)$ obtained at the preceding iteration step is already sufficiently small. This algorithm is described in the Appendix of the present paper. In the sequel, we will denote the function $S_s(R)$ constructed according to the algorithm of Ref. [1] by $S_s^*(R)$. The matrix $S_s^*$ tends to the identity matrix as the coupling $\Pi_s$ vanishes.

## *Classical path approach*

Another important property of the post-adiabatic approach is the absence of an adequate analogue for the classical path approximation (11). The reason is mainly a more complicated structure of the post-adiabatic couplings $\Pi_s$ of orders $s \geqslant 1$ compared with the usual nonadiabatic coupling $\Pi_0$ [Eq. (16)]. As a natural attempt to the post-adiabatic generalization for the classical path approximation we may propose the following construction. Let $\mathcal{F}_E$ be some continuous operator mapping an $R$-dependent Hamiltonian matrix $K(R)$ of order $2N$ into an $R$-dependent symmetric matrix $\mathcal{F}_E[K](R)$ of order $N$, the following two conditions being satisfied:

(a) If $\pm\lambda_1, \ldots, \pm\lambda_N$ are the eigenvalues of the matrix $K$ then $\lambda_1^2 + E, \ldots, \lambda_N^2 + E$ are the eigenvalues of the matrix $\mathcal{F}_E[K]$.

(b)
$$\mathcal{F}_E\left[\begin{pmatrix} 0 & I \\ V & 0 \end{pmatrix}\right] = V + EI$$

for any symmetric matrix $V$ of order $N$ (recall that $I$ denotes the identity $N \times N$ matrix).

These two conditions are consistent because the eigenvalues of the Hamiltonian matrix entering condition (b) are equal to $\pm u_k^{1/2}$ where $u_k$ are the eigenvalues of $V$.

Then the post-adiabatic classical path approximation of order $s + 1 \geqslant 1$ corresponding to the total energy $E$ can be defined as the equation

$$i\hbar \frac{\partial \Psi_{s+1}}{\partial t} = H_{s+1} \Psi_{s+1},$$

where $H_{s+1} = H_{s+1}(r; R(t))$ is a linear operator in the $N$-dimensional space (of scalar functions in $r$) whose matrix in a certain $R$-independent orthonormalized basis is equal to $\mathcal{F}_E[K_s(R(t))]$, $K_s(R)$ being matrix (18). One may assume the function $R(t)$ to satisfy the same Eq. (14) as in the case of the usual classical path approximation.

The main difficulty in this program is again nonuniqueness, since the operator $\mathcal{F}_E$ can be chosen in many ways.

### *Energy dependence*

For $s \geqslant 1$ the post-adiabatic potentials $u_k^{(s)}(R)$ and couplings $\Pi_s(R)$ depend upon the total energy $E$ of the system. However, as we will see in Sect. 7, for many systems, this dependence turns out to be rather weak in the physically interesting range of $E$.

### *Complex potentials and couplings*

The post-adiabatic iterations can lead to complex potentials and couplings.

First, the real Hamiltonian matrix $K_s$ [Eq. (18)] may well possess not only real pairs $\pm\lambda$ of eigenvalues (corresponding to "classically forbidden" states $u_k^{(s+1)} = \lambda^2 + E > E$) and purely imaginary pairs $\pm i\omega$ (corresponding to "classically accessible" states $u_k^{(s+1)} = E - \omega^2 < E$) but also quadruplets $\pm\alpha \pm i\beta$ of eigenvalues ($\alpha > 0$, $\beta > 0$). Each such quadruplet gives rise to two complex-conjugated potentials $u_{k,k+1}^{(s+1)} = \alpha^2 - \beta^2 + E \pm 2i\alpha\beta$. The physical meaning of complex post-adiabatic potentials in the Klar–Fano construction requires further investigation: unitarity is lost when the potential is complex and couplings are neglected. In the weak coupling cases investigated so far the problem is negligible. Imaginary (optical) potentials are widely used in the theory of inelastic processes and chemical reactions [31, 32], where they are introduced *ad hoc* to model the loss of probability conservation. Therefore it would be interesting to see whether imaginary terms which arise in this theory can be similarly interpreted as effective "optical" potentials, and so be useful to estimate the probability loss associated with interchannel coupling.

Second, even if all the eigenvalues of the real matrix $K_s$ [Eq. (18)] are either real or purely imaginary and the matrix (19) is therefore real, a symplectic operator $S_s$ conjugating these two matrices cannot always be chosen to be real. This has been explained in more detail in Ref. [1]. If the matrix $S_s$ is not real then the coupling $\Pi_{s+1}$ [Eq. (21)] and the matrix $K_{s+1}$ to be handled at the next iteration step will not, generally speaking, be real.

Luckily, both these difficulties disappear when the coupling $\Pi_s$ is small. To be more precise, if the post-adiabatic potentials $u_1^{(s)}, \dots, u_N^{(s)}$ of order $s$ are real, distinct, and other than $E$ and the post-adiabatic coupling $\Pi_s$ of order $s$ is real and sufficiently small, then the post-adiabatic potentials $u_1^{(s+1)}, \dots, u_N^{(s+1)}$ of order $s+1$ are real and the matrix $S_s$ can be also chosen to be real. In particular, the algorithm of Ref. [1] gives the real matrix $S_s^*$. In practice, "sufficiently small coupling" usually means "not very strong one". For all the systems O, F, Cl–He, Ne, Ar, Kr, Xe, $D_2$, $CH_4$, HCl, HBr, HI considered in Sect. 7 (except for O–He) the post-adiabatic potentials $u_k^{(1)}$ for all the values of $R$ turn out to be real for physically interesting energies $E$ and the matrix $S_0$ can be also chosen to be real. This leads to a real post-adiabatic coupling $\Pi_1$.

## *Comparison of couplings*

The usual nonadiabatic coupling in an $N$-state system with the only "slow" coordinate $R$ is described by the skew-symmetric $N \times N$ matrix $P$ whose elements have the dimension of length$^{-1}$ according to Eq. (9). On the other hand, the post-adiabatic couplings $\Pi_s$ of orders $s \geqslant 1$ are Hamiltonian $2N \times 2N$ matrices

$$\Pi_s = \begin{pmatrix} A_s & B_s \\ C_s & -A_s^t \end{pmatrix},$$

$A_s$ being an $N \times N$ matrix without any special symmetry properties whereas $B_s$ and $C_s$ are symmetric $N \times N$ matrices. Recall that the upper index t means a transposed matrix. What is of great importance for the post-adiabatic approach is that the elements of the blocks $A_s$, $B_s$, $C_s$ are of different dimensions:

$$\Pi_s \sim \begin{pmatrix} \text{length}^{-1} & \text{length}^{-1}\text{energy}^{-1/2} \\ \text{length}^{-1}\text{energy}^{1/2} & \text{length}^{-1} \end{pmatrix}.$$

The elements of the $N \times N$ blocks of the matrices $K_s$ and $S_s$ for each $s \geqslant 0$ are also of different dimensions:

$$K_s \sim \begin{pmatrix} \text{energy}^{1/2} & 1 \\ \text{energy} & \text{energy}^{1/2} \end{pmatrix}, \qquad S_s \sim \begin{pmatrix} 1 & \text{energy}^{-1/2} \\ \text{energy}^{1/2} & 1 \end{pmatrix}.$$

To compare $\Pi_s$ ($s \geqslant 1$) and $P$, it is necessary to multiply the elements of the blocks $B_s$ and $C_s$ of the matrix $\Pi_s$ by some functions in the adiabatic potentials $u_1, \dots, u_N$ to achieve the dimension of length$^{-1}$.

*Noncrossing rule*

The noncrossing rule for the terms of the same symmetry [5] undergoes a marked modification when applied to the post-adiabatic potentials. This fact is closely connected with the possibility of complex potentials and is explained in detail in the next section.

## 6 The two-state problem

As the simplest example, consider the case $N = 2$ (the two-state problem). The importance of this case stems not only from the fact that many characteristics of the process with $N = 2$ states can be calculated analytically, but mainly from the fact that the nonadiabatic transitions in a system with any number $N$ of states can often be approximately described within the two-state model [5]. For any $N$, each element $P_{kl} = -P_{lk}$ of the coupling matrix $P(R)$ is, as a rule, of a noticeable magnitude only for the values of the "slow" coordinate $R$ ranging in a rather narrow interval [e.g., near the avoided crossing point, i.e., the point of the minimal splitting of the adiabatic potentials $u_k(R)$ and $u_l(R)$]. The other elements of the matrix $P(R)$ are small in this interval, in particular, what is most important is that the elements $P_{km}$ for $m \neq l$ and $P_{lm}$ for $m \neq k$ are small. The situation where for some value of $R$ all the three pairwise couplings between three states $\varphi_k$, $\varphi_l$, and $\varphi_m$ are strong occurs rarely. In studies of the nonadiabatic transitions $k \leftrightarrow l$, it is therefore often possible to confine oneself to considering two potentials $u_k(R)$, $u_l(R)$ only and the coupling $P_{kl}(R)$ between them (if the neighboring avoided crossing points do not lie too close to the one corresponding to the states $\varphi_k$ and $\varphi_l$). Note that this conclusion is in fact valid for any number of "slow" coordinates $R_\alpha$.

Besides that, in some problems involving, at first glance, $N \geqslant 3$ pairwise coupled states, the latter are divided into noninteracting groups of one or two states. This is just the situation for the systems O–He, Ne, Ar, Kr, Xe, $D_2$, $CH_4$ considered in the next section.

In the dimension $N = 2$, the matrix $P$ of the nonadiabatic coupling [Eq. (9)] takes the form

$$P = \begin{pmatrix} 0 & p \\ -p & 0 \end{pmatrix}$$

and the full matrix $K_0$ [Eq. (22)], the form

$$K_0 = \begin{pmatrix} 0 & a & 1 & 0 \\ -a & 0 & 0 & 1 \\ \sigma + \tau & 0 & 0 & a \\ 0 & \sigma - \tau & -a & 0 \end{pmatrix}, \qquad a = \frac{\hbar p}{\sqrt{2M}}, \tag{23}$$

where $\sigma = \frac{1}{2}(u_1 + u_2) - E$ and $\tau = \frac{1}{2}(u_1 - u_2) > 0$ (recall that $u_1$ and $u_2$ denote the usual adiabatic potentials). The two-state problem is therefore characterized by three energy-dimensional functions $\sigma(R) = \sigma_E(R)$, $\tau(R)$, and $\gamma(R)$, where $\gamma = a^2 > 0$. The first-order post-adiabatic potentials corresponding to the total energy $E$ are

$$u_1^{(1)} = \sigma - \gamma + (\tau^2 - 4\sigma\gamma)^{1/2} + E, \qquad u_2^{(1)} = \sigma - \gamma - (\tau^2 - 4\sigma\gamma)^{1/2} + E. \tag{24}$$

**Table 1.** The evolution of the first-order post-adiabatic potentials $u_1^{(1)}$ and $u_2^{(1)}$ for $\sigma, \tau$ fixed and $\gamma$ increasing. Note that $-\sigma - \tau = E - u_1$, $\tau - \sigma = E - u_2$, $\tau^2/4\sigma = (u_1 - u_2)^2/8(u_1 + u_2 - 2E)$, where $u_1 > u_2$ are the usual adiabatic potentials. An asterisk in the last column means that the symplectic matrix $S_0$ cannot be chosen to be real although $u_1^{(1)}$ and $u_2^{(1)}$ are real

| Relations between $u_1$, $u_2$, and $E$; here $\kappa = (u_1 - E)/(E - u_2)$ | The $\gamma$ range | Relations between $u_1^{(1)}$, $u_2^{(1)}$, and $E$ | |
|---|---|---|---|
| $\sigma < 0$, $0 < \tau < -\sigma$,<br>i.e., $u_2 < u_1 < E$ | $0 < \gamma < -\sigma - \tau$ | $u_2^{(1)} < u_1^{(1)} < E$ | |
| | $-\sigma - \tau < \gamma < \tau - \sigma$ | $u_2^{(1)} < E < u_1^{(1)}$ | |
| | $\gamma > \tau - \sigma$ | $u_2^{(1)} < u_1^{(1)} < E$ | * |
| $\sigma < 0$, $\tau \geqslant -\sigma$,<br>i.e., $u_2 < E \leqslant u_1$, $\kappa < 1$ | $0 < \gamma < \tau - \sigma$ | $u_2^{(1)} < E < u_1^{(1)}$ | |
| | $\gamma > \tau - \sigma$ | $u_2^{(1)} < u_1^{(1)} < E$ | * |
| $\sigma > 0$, $\tau > 2\sigma$,<br>i.e., $u_2 < E < u_1$, $1 < \kappa < 3$ | $0 < \gamma < \tau - \sigma$ | $u_2^{(1)} < E < u_1^{(1)}$ | |
| | $\tau - \sigma < \gamma < \tau^2/(4\sigma)$ | $u_2^{(1)} < u_1^{(1)} < E$ | * |
| | $\gamma > \tau^2/(4\sigma)$ | $u_1^{(1)}$ and $u_2^{(1)}$ are complex | |
| $\sigma > 0$, $\sigma < \tau < 2\sigma$,<br>i.e., $u_2 < E < u_1$, $\kappa > 3$ | $0 < \gamma < \tau - \sigma$ | $u_2^{(1)} < E < u_1^{(1)}$ | |
| | $\tau - \sigma < \gamma < \tau^2/(4\sigma)$ | $E < u_2^{(1)} < u_1^{(1)}$ | |
| | $\gamma > \tau^2/(4\sigma)$ | $u_1^{(1)}$ and $u_2^{(1)}$ are complex | |
| $\sigma > 0$, $0 < \tau \leqslant \sigma$,<br>$E \leqslant u_2 < u_1$ | $0 < \gamma < \tau^2/(4\sigma)$ | $E < u_2^{(1)} < u_1^{(1)}$ | |
| | $\gamma > \tau^2/(4\sigma)$ | $u_1^{(1)}$ and $u_2^{(1)}$ are complex | |

If $\sigma > 0$ and $\gamma > \tau^2/(4\sigma)$, then these potentials are not real. So, complex post-adiabatic potentials do not occur for "classically accessible" motions (where $u_1 < E$, $u_2 < E$, and therefore $\sigma < 0$) and are typical for "strongly classically forbidden" regions ($u_1 \gg E$, $u_2 \gg E$) with a considerable coupling.

Some features of the evolution of $u_1^{(1)}$ and $u_2^{(1)}$ for $u_1 - E$, $u_2 - E$ fixed (i.e., $\sigma, \tau$ fixed) and the coupling $p$ increasing [i.e., the parameter $\gamma = \hbar^2 p^2/(2M)$ increasing] are presented in Table 1 (recall that we have set $u_1 > u_2$).

The algorithm of Ref. [1] leads to the following matrix $S_0$:

$$S_0 = S_0^* = \begin{pmatrix} \rho_{11} & 0 & 0 & \rho_{14} \\ 0 & \rho_{22} & \rho_{23} & 0 \\ 0 & \rho_{32} & \rho_{33} & 0 \\ \rho_{41} & 0 & 0 & \rho_{44} \end{pmatrix},$$

where

$$\rho_{11} = (u_1^{(1)} - \gamma - \sigma + \tau - E)/D_1, \qquad \rho_{22} = (u_2^{(1)} - \gamma - \sigma - \tau - E)/D_2,$$
$$\rho_{23} = -2a/D_1, \quad \rho_{14} = 2a/D_2,$$
$$\rho_{41} = -a(u_1^{(1)} + \gamma + \sigma - \tau - E)/D_1, \quad \rho_{32} = a(u_2^{(1)} + \gamma + \sigma + \tau - E)/D_2,$$
$$\rho_{33} = (u_1^{(1)} + \gamma - \sigma + \tau - E)/D_1, \qquad \rho_{44} = (u_2^{(1)} + \gamma - \sigma - \tau - E)/D_2$$

and

$$D_1 = \{2(\tau^2 - 4\sigma\gamma)^{1/2}[(\tau^2 - 4\sigma\gamma)^{1/2} + \tau - 2\gamma]\}^{1/2},$$
$$D_2 = -\{2(\tau^2 - 4\sigma\gamma)^{1/2}[(\tau^2 - 4\sigma\gamma)^{1/2} + \tau + 2\gamma]\}^{1/2}.$$

Recall that $a = \sqrt{\gamma} = \hbar p/\sqrt{2M}$. When the matrix $S_0$ can be chosen to be real, the algorithm of Ref. [1] does present a real matrix $S_0^*$.

For $S_0 = S_0^*$ the first-order post-adiabatic coupling takes the form

$$\Pi_1 = (S_0^*)^{-1} \frac{dS_0^*}{dR} = \begin{pmatrix} x & 0 & 0 & z \\ 0 & y & z & 0 \\ 0 & t & -x & 0 \\ t & 0 & 0 & -y \end{pmatrix}.$$

The easiest way to calculate the elements $x, y, z$, and $t$ is as follows. The matrix $(S_0^*)^{-1}(dK_0/dR)S_0^*$ with $K_0$ the operator [Eq. (23)] is Hamiltonian at each value of $R$. This matrix has therefore the form

$$(S_0^*)^{-1} \frac{dK_0}{dR} S_0^* = \begin{pmatrix} A & B \\ C & -A^t \end{pmatrix},$$

where $A$, $B$, and $C$ are $2 \times 2$ matrices, $B$ and $C$ being symmetric. If $A_{ij}$, $B_{ij}$, and $C_{ij}$ are the elements of the matrices $A$, $B$, and $C$, respectively ($i, j = 1, 2$), then

$$x = \frac{B_{11}}{2}, \quad y = \frac{B_{22}}{2}, \quad z = \frac{A_{12} - A_{21}}{u_2^{(1)} - u_1^{(1)}}, \quad t = \frac{(u_1^{(1)} - E)A_{12} - (u_2^{(1)} - E)A_{21}}{u_2^{(1)} - u_1^{(1)}}. \quad (25)$$

Formulas (25) are a particular case of the so-called symplectic Hellmann–Feynman theorem [1]. These formulas enable one to find the post-adiabatic coupling $\Pi_1$ without differentiating the operator $S_0^*$.

As already mentioned in the previous section, the functions $x(R)$, $y(R)$, $z(R)$, and $t(R)$ are of dimensions

$$x \sim y \sim \text{length}^{-1}, \qquad z \sim \text{length}^{-1}\ \text{energy}^{-1/2}, \qquad t \sim \text{length}^{-1}\ \text{energy}^{1/2}.$$

To compare $\Pi_1$ with $\Pi_0$ (i.e., $x, y, z$, and $t$ with $p$) it is therefore necessary to correct the elements $z$ and $t$ dimensionally. Below, while analyzing the systems O, F, Cl–He, Ne, Ar, Kr, Xe, $D_2$, $CH_4$, HCl, HBr, HI, we compare $p$ with the functions

$$x, y, \tilde{z} = \Delta z, \qquad \tilde{t} = \frac{t}{\Delta}, \tag{26}$$

where

$$\Delta = [\tfrac{1}{2}(u_1 - u_2)]^{1/2}. \tag{27}$$

Using the two-state problem as an example, it is easy to explain the post-adiabatic analogue of the noncrossing rule for the terms of the same symmetry. Set $p = \text{const.}$ (so that $\gamma = \text{const.}$) and

$$u_1 = \alpha R^2 + \beta + \gamma, \qquad u_2 = \gamma - \alpha R^2 - \beta,$$

where $\alpha$ and $\beta$ are some positive constants of dimensions

$$\alpha \sim \text{length}^{-2}\ \text{energy}, \qquad \beta \sim \text{energy}.$$

Then $\sigma = \gamma - E$ and $\tau = \alpha R^2 + \beta$. The first-order post-adiabatic potentials (24) are

$$u_{1,2}^{(1)}(R) = \pm[(\alpha R^2 + \beta)^2 + 4(E - \gamma)\gamma]^{1/2}.$$

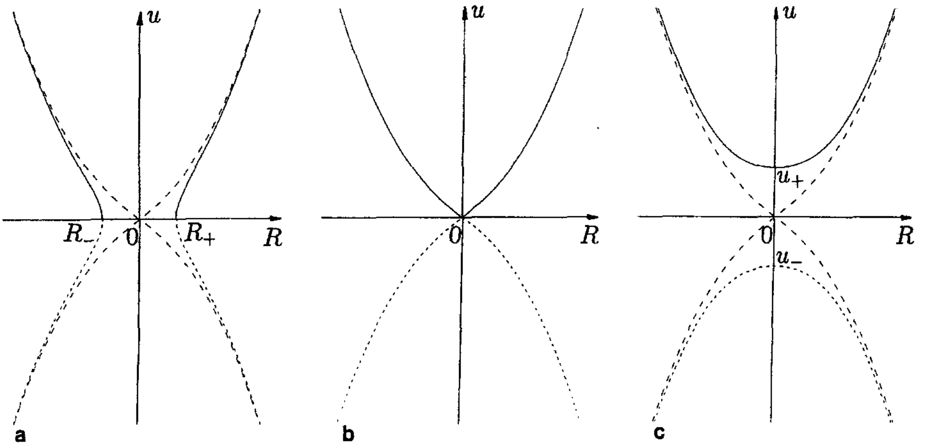

$E < \dfrac{4\gamma^2 - \beta^2}{4\gamma}$ $E = \dfrac{4\gamma^2 - \beta^2}{4\gamma}$ $E > \dfrac{4\gamma^2 - \beta^2}{4\gamma}$

**Fig. 1a–c.** The first-order post-adiabatic potentials $u_1^{(1)}$ (shown by the solid line) and $u_2^{(1)}$ (shown by the dotted line) in a two-state problem with the adiabatic potentials $u_1 = \alpha R^2 + \beta + \gamma$, $u_2 = \gamma - \alpha R^2 - \beta$ [$\alpha$, $\beta$, and $\gamma = \hbar^2 p^2/(2M)$ being constants]. The potentials $u_{1,2}^{(1)}$ for the critical value $(4\gamma^2 - \beta^2)/(4\gamma)$ of the total energy $E$ (panel b) are also plotted in panels a and c by the dashed line. The values $R_-$ and $R_+$ of the coordinate $R$ in panel a are coalescence points

These potentials are plotted in Fig. 1 for various values of the total energy $E$ ($u_1^{(1)}$ is shown by a solid line and $u_2^{(1)}$ by a dotted one). The quantities $R_\pm$ in Fig. 1a and $u_\pm$ in Fig. 1c are

$$R_\pm = \pm\left(\frac{2[\gamma(\gamma - E)]^{1/2} - \beta}{\alpha}\right)^{1/2}, \qquad u_\pm = \pm[\beta^2 + 4(E - \gamma)\gamma]^{1/2}.$$

The dashed line in Figs. 1a, c shows the potentials $u_{1,2}^{(1)}$ for the critical value $E = (4\gamma^2 - \beta^2)/(4\gamma)$ of the total energy:

$$u_{1,2}^{(1)}(R)_{\text{crit}} = \pm R[\alpha^2 R^2 + 2\alpha\beta]^{1/2}.$$

The values $R_-$ and $R_+$ of the coordinate $R$ in Fig. 1a are coalescence points. At these points, $u_1^{(1)} = u_2^{(1)}$, while the potentials $u_1^{(1)}$ and $u_2^{(1)}$ are complex for $R_- < R < R_+$.

Another type of coalescence point evolution is observed for a two-state problem with $\gamma = \text{const.}$ and

$$u_1 = \gamma + (\alpha R^2 + \beta)^{-1}, \qquad u_2 = \gamma - (\alpha R^2 + \beta)^{-1},$$

where $\alpha$ and $\beta$ are some positive constants of dimensions

$$\alpha \sim \text{length}^{-2}\ \text{energy}^{-1}, \qquad \beta \sim \text{energy}^{-1}.$$

Then $\sigma = \gamma - E$ and $\tau = (\alpha R^2 + \beta)^{-1}$. The first-order post-adiabatic potentials (24) are

$$u_{1,2}^{(1)}(R) = \pm[(\alpha R^2 + \beta)^{-2} + 4(E - \gamma)\gamma]^{1/2}.$$

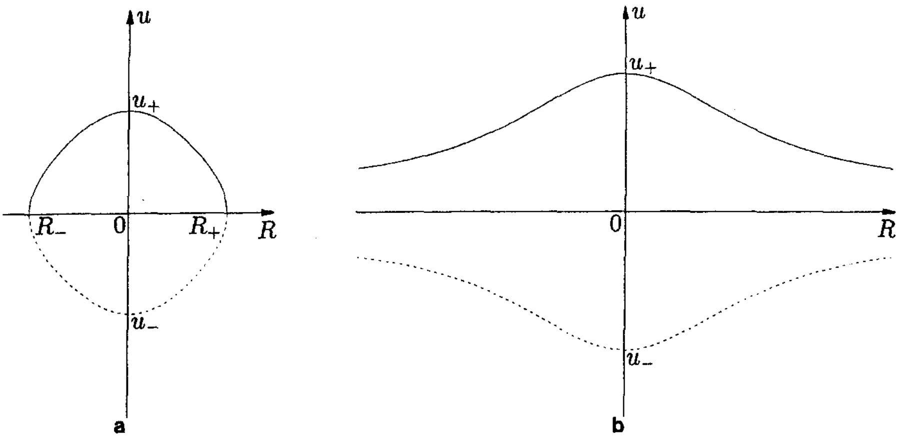

$\frac{4\gamma^2-\beta^{-2}}{4\gamma} < E < \gamma$

$E \geq \gamma$

Fig. 2. The first-order post-adiabatic potentials $u_1^{(1)}$ (shown by the solid line) and $u_2^{(1)}$ (shown by the dotted line) in a two-state problem with the adiabatic potentials $u_1 = \gamma + (\alpha R^2 + \beta)^{-1}$, $u_2 = \gamma - (\alpha R^2 + \beta)^{-1}$ [$\alpha$, $\beta$, and $\gamma = \hbar^2 p^2/(2M)$ being constants]. The values $R_-$ and $R_+$ of the coordinate $R$ in panel a are coalescence points

For $E \leqslant (4\gamma^2 - \beta^{-2})/(4\gamma)$ these potentials are complex for all $R$. For $E > (4\gamma^2 - \beta^{-2})/(4\gamma)$ the potentials $u_{1,2}^{(1)}(R)$ are plotted in Fig. 2 ($u_1^{(1)}$ is shown by a solid line and $u_2^{(1)}$ by a dotted one). The quantities $R_\pm$ in Fig. 2a and $u_\pm$ in Figs. 2a, b are

$$R_\pm = \pm\left(\frac{[4\gamma(\gamma - E)]^{-1/2} - \beta}{\alpha}\right)^{1/2}, \qquad u_\pm = \pm[\beta^{-2} + 4(E - \gamma)\gamma]^{1/2}.$$

These values $R_-$ and $R_+$ of the coordinate $R$ in Fig. 2a are coalescence points. At these points, $u_1^{(1)} = u_2^{(1)}$, while the potentials $u_1^{(1)}$ and $u_2^{(1)}$ are complex for $R < R_-$ and $R > R_+$.

It turns out that for any irreducible generic system with any number $N$ of states, the singularities of the post-adiabatic potentials $u_k^{(s)}$ of any order $s \geqslant 1$ are the same as in these model examples (irreducibility means that the states cannot be divided into several noninteracting groups). Namely, at almost all the values of the energy $E$ the potentials $u_k^{(s)}$ and $u_l^{(s)}$ do not intersect except for coalescence points where these potentials possess a square root singularity, see Fig. 3a. At some isolated values of $E$ the potentials $u_k^{(s)}$ and $u_l^{(s)}$ constitute two smooth curves intersecting at a nonzero angle, see Fig. 3b. The metamorphoses of these potentials as $E$ passes through the critical value look the same as in Figs. 1a, b, c.

## 7 Van der Waals interactions of O, F and Cl atoms with closed shell systems

As an application, consider the long-range interaction of $^2P$ and $^3P$ atoms with a closed shell system, e.g., a $^1S$ atom.

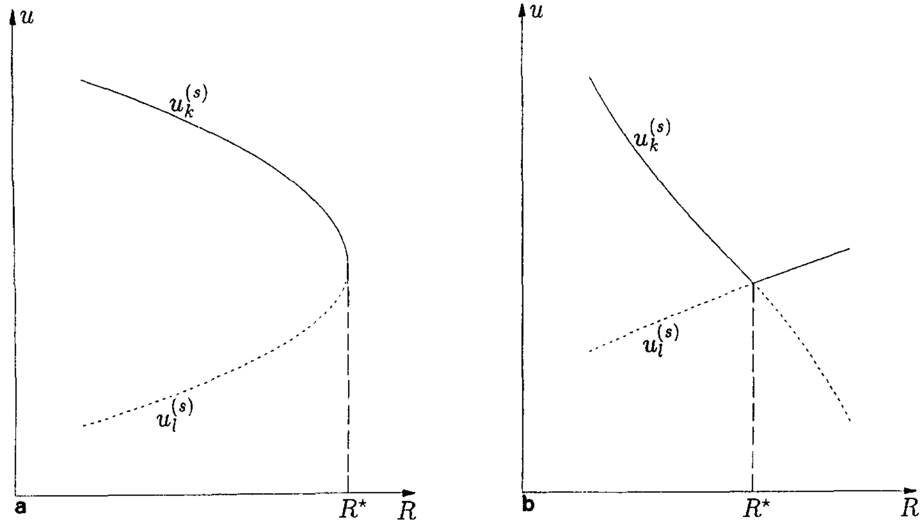

**Fig. 3.** Typical singularities of the post-adiabatic potentials. The values $R^*$ of the coordinate $R$ are coalescence points

When a $^1S$ particle approaches a $^2P$ particle, the $^2P_{3/2}$ state of the latter gives rise to two molecular terms

$$V_{3/2,\Omega}(R), \qquad \Omega = 1/2, 3/2,$$

while the $^2P_{1/2}$ state gives rise to only one term

$$V_{1/2,1/2}(R),$$

$R$ being the internuclear distance [33]. The radial relative motion of the particles induces transitions between the states with the same projection $\Omega$ of the electronic total angular momentum along the $R$ axis, i.e., the transitions

$$|3/2, 1/2\rangle \Leftrightarrow |1/2, 1/2\rangle.$$

There is no coupling between the $|3/2, 3/2\rangle$ state and the two states with $\Omega = 1/2$. The latter ones (i.e., the $|3/2, 1/2\rangle$ and $|1/2, 1/2\rangle$ states) are coupled, and they constitute a two-state problem which is of our interest in the sequel.

For the interaction of a $(p^5)(^2P)$ atom (e.g., a halogen atom) with a $^1S$ particle, the $|3/2, 1/2\rangle$ state is the ground one [33]. It correlates with the ground $^2P_{3/2}$ state of the $(p^5)(^2P)$ atom as $R \to \infty$. As $R \to 0$, when the spin–orbit interaction energy $V_{so}$ becomes small compared with the orbit–axis interaction energy $V_{el}$, the states

$$|3/2, 1/2\rangle, \quad |3/2, 3/2\rangle, \quad |1/2, 1/2\rangle$$

can be identified as

$$^2\Sigma^+_{1/2}, \quad ^2\Pi_{3/2}, \quad ^2\Pi_{1/2},$$

respectively [33]. Rotations of the molecular axis mix the states with $\Omega = 1/2$ and $\Omega = 3/2$.

When a $^1S$ particle approaches a $^3P$ particle, the $^3P_2$ state of the latter gives rise to three molecular terms

$$V_{2\Omega}(R), \quad \Omega = 0, 1, 2,$$

the $^3P_1$ state, to two terms

$$V_{1\Omega}(R), \quad \Omega = 0, 1,$$

and the $^3P_0$ state, to one term

$$V_{00}(R),$$

see Ref. [33]. The radial relative motion of the particles induces transitions between the states with the same value of $\Omega$. The six components of the fine $^3P$–$^1S$ structure are therefore divided into three noninteracting groups:

the states with $\Omega = 0$: $|0\,0\rangle, |1\,0\rangle, |2\,0\rangle$;
the states with $\Omega = 1$: $|1\,1\rangle, |2\,1\rangle$;
the state with $\Omega = 2$: $|2\,2\rangle$.

However, actual calculations show [33] that the coupling between the state $|1\,0\rangle$ and the states $|0\,0\rangle$, $|2\,0\rangle$ also vanishes. Thus, all the possible transitions between the fine structure components which are induced by the radial relative motion of the particles are

$$|0\,0\rangle \Leftrightarrow |2\,0\rangle, \qquad |1\,1\rangle \Leftrightarrow |2\,1\rangle.$$

The two pairs of states $|0\,0\rangle, |2\,0\rangle$ and $|1\,1\rangle$, $|2\,1\rangle$ constitute two two-state problems which are of our interest in the sequel.

For the interaction of a $(p^4)(^3P)$ atom (e.g., an oxygen, sulfur, selenium, or tellurium atom) with a $^1S$ particle, the $|2\,2\rangle$ state is the ground one [33]. It correlates with the ground $^3P_2$ state of the $(p^4)(^3P)$ atom as $R \to \infty$. As $R \to 0$, the states

$$|2\,2\rangle, \quad |2\,1\rangle, \quad |2\,0\rangle, \quad |1\,0\rangle, \quad |1\,1\rangle, \quad |0\,0\rangle$$

can be identified as

$$^3\Pi_2, \quad ^3\Pi_1, \quad ^3\Pi_0, \quad ^3\Pi_0, \quad ^3\Sigma_1^-, \quad ^3\Sigma_0^-,$$

respectively. Note a misprint in Fig. 2 of Ref. [33] concerning this problem: the letters $\Sigma$ and $\Pi$ on the fourth plot (from the top) in the right column should be interchanged. Rotations of the molecular axis mix the states with different values of $\Omega$.

In the present paper, we neglect the molecular axis rotation effects and treat the internuclear distance $R$ as the only "slow" coordinate. This enables one to apply the post-adiabatic analysis to the interactions $^2P$–$^1S$ and $^3P$–$^1S$.

The adiabatic potentials $V_{j\Omega}(R)$ and the element $p(R)$ of the matrix of nonadiabatic coupling between the $|3/2, 1/2\rangle$ and $|1/2, 1/2\rangle$ states have been determined for the 17 $^2P$–$^1S$ systems F, Cl–He, Ne, Ar, Kr, Xe, $D_2$, $CH_4$ (see Ref. [34] for F and Ref. [35] for Cl) and F–HCl, HBr, HI [36]. The adiabatic potentials $V_{j\Omega}(R)$, the element $p_0(R)$ of the matrix of nonadiabatic coupling between the $|2\,0\rangle$ and $|0\,0\rangle$ states, and the element $p_1(R)$ of the matrix of nonadiabatic coupling between the $|2\,1\rangle$ and $|1\,1\rangle$ states have been determined for the seven $^3P$–$^1S$ systems O–He, Ne, Ar, Kr, Xe, $D_2$, $CH_4$ [37]. In all the cases, those features of the van der

Waals intermolecular interaction were found by analyzing the differential and total cross-sections for elastic scattering in crossed molecular beam experiments (the $D_2, CH_4, HCl, HBr$, and HI molecules were treated as spherically symmetric $^1S$ particles). The applications are exemplified by evaluating the transport cross-sections and therefore collision integrals for the F–Xe and O–He systems [38].

For all these systems for $1 \leqslant R \leqslant 7$ Å, we have calculated, by formulas (24)–(25) of the previous section, the first-order post-adiabatic potentials and coupling matrices corresponding to the total energy $E = -50, 25$, and 100 meV. In fact, for the F–HCl, HBr, HI interactions, the potentials $u_1^{(1)}$, $u_2^{(1)}$ and coupling matrices $\Pi_1$ corresponding to $E = 25$ meV were reported in Ref. [1]. The values $E = 25$ meV and $E = 100$ meV lie in the experimentally observable range. The reduced mass $\mu$ of the two particles was used for $M$. The matrix $S_0 = S_0^*$ was constructed by the algorithm of Ref. [1]. The main results of our computations are presented in Tables 2–5 referring to the states of the system F–$^1S$ with $\Omega = 1/2$, those of the systems Cl–$^1S$ with $\Omega = 1/2$, those of the system O–$^1S$ with $\Omega = 0$, and those of the systems O–$^1S$ with $\Omega = 1$.

In these tables, the following notations are used. For any function $f$ of the internuclear distance $R$, we denote by $R_f$ the point where the absolute value $|f|$ of this function attains a maximum.

In the first and second columns of the tables, we point out the distance $R_p$ where the absolute value of the element $p(R)$ of the nonadiabatic coupling matrix attains a maximum, and the maximal value $|p(R_p)|$ itself.

Some characteristics of the functions $x, y, \tilde{z}, \tilde{t}$ [Eq. (26)] describing the first-order post-adiabatic coupling $\Pi_1$ are given in the columns 4–7. In the fourth column, we present the distance $R_{x,y}$ equal to $R_x$ if the maximum of $|x(R)|$ is greater than the maximum of $|y(R)|$, and to $R_y$ otherwise. The value of the function $x$ (or $y$) itself at $R = R_{x,y}$ is pointed out in the fifth column. Similarly, in the sixth column, we present the distance $R_{\tilde{z},\tilde{t}}$ equal to $R_{\tilde{z}}$ if the maximum of $|\tilde{z}(R)|$ is greater than the maximum of $|\tilde{t}(R)|$, and to $R_{\tilde{t}}$ otherwise. The value of the function $\tilde{z}$ (or $\tilde{t}$) itself at $R = R_{\tilde{z},\tilde{t}}$ is pointed out in the seventh column.

The last two columns refer to the differences $\delta_1 = u_1 - u_1^{(1)}$ and $\delta_2 = u_2 - u_2^{(1)}$ of the adiabatic and first-order post-adiabatic potentials. In the eighth column, we give the distance $R_*$ where the function $\max(|\delta_1(R)|, |\delta_2(R)|)$ attains a maximum. The difference $\delta_1(R_*)$ or $\delta_2(R_*)$ itself is pointed out in the ninth column (we present the difference whose absolute value is larger). This difference should be compared with the potential well depth $\varepsilon$ of the curve $u_2(R)$ given in the second column (the minimum position $R_0$ for this curve is pointed out in the first column).

In all the four tables, the systems are ordered according to the potential well depth of the ground state ($V_{3/2,1/2}$ for the F–$^1S$ and Cl–$^1S$ systems and $V_{22}$ for the O–$^1S$ systems): the well depth increases from top to bottom. The minimum position $\overline{R_0}$ and the potential well depth $\bar{\varepsilon}$ of the curve $V_{22}(R)$ for the O–$^1S$ systems are collected in Table 6.

Note that for all the three series F–$^1S$, Cl–$^1S$, and O–$^1S$, placing the systems according to the increase of the potential well depth of the ground state leads to the same order of the target molecules:

$$\text{He–Ne–D}_2\text{–Ar–(HCl)–(HBr)–Kr–CH}_4\text{–(HI)–Xe} \tag{28}$$

(the molecules whose interaction with the fluorine atom only has been studied are put in parentheses).

**Table 2.** Some characteristic features of the first-order post-adiabatic potentials and couplings for the F–$^1S$ systems. For the notations, see the text. The quantities $R_0$ and $\varepsilon$ refer to $u_2 = V_{3/2,1/2}$

| System<br>$R_p$ (Å)<br>$R_0$ (Å) | <br>$\lvert p\rvert$ (Å$^{-1}$)<br>$\varepsilon$ (meV) | $E$ (meV) | $R_{x,y}$ (Å) | $x$ or $y$ (Å$^{-1}$) | $R_{\tilde{z},\tilde{t}}$ (Å) | $\tilde{z}$ or $\tilde{t}$ (Å$^{-1}$) | $R_*$ (Å) | $\delta_1$ or $\delta_2$ (meV) |
|---|---|---|---|---|---|---|---|---|
| F–He | | −50 | 1.62 | $y = 0.380$ | 1.73 | $\tilde{t} = 5.99$ | 1.56 | $\delta_1 = 12.0$ |
| 1.65 | 0.614 | 25 | 1.61 | $y = 0.362$ | 1.72 | $\tilde{t} = 5.82$ | 1.54 | $\delta_1 = 11.2$ |
| 3.01 | 2.20 | 100 | 1.61 | $y = 0.346$ | 1.70 | $\tilde{t} = 5.73$ | 1.53 | $\delta_1 = 10.4$ |
| F–Ne | | −50 | 2.33 | $y = 0.0173$ | 2.49 | $\tilde{t} = 0.384$ | 2.31 | $\delta_1 = 0.783$ |
| 2.39 | 0.627 | 25 | 2.32 | $y = 0.0172$ | 2.42 | $\tilde{t} = 0.465$ | 2.24 | $\delta_1 = 0.564$ |
| 3.02 | 5.65 | 100 | 2.32 | $y = 0.0171$ | 2.38 | $\tilde{t} = 0.600$ | 2.16 | $\delta_1 = 0.420$ |
| F–$D_2$ | | −50 | 2.53 | $y = 0.0203$ | 2.94 | $\tilde{t} = 0.359$ | 2.63 | $\delta_1 = 1.45$ |
| 2.62 | 0.626 | 25 | 2.53 | $y = 0.0198$ | 2.44 | $\tilde{z} = -0.228$ | 2.50 | $\delta_1 = 0.602$ |
| 3.13 | 6.05 | 100 | 2.52 | $y = 0.0195$ | 2.56 | $\tilde{t} = 0.473$ | 2.73 | $\delta_2 = 1.04$ |
| F–Ar | | −50 | 2.73 | $y = 0.00467$ | 3.13 | $\tilde{t} = 0.176$ | 2.81 | $\delta_1 = 0.374$ |
| 2.80 | 0.632 | 25 | 2.73 | $y = 0.00464$ | 2.63 | $\tilde{z} = -0.117$ | 2.71 | $\delta_1 = 0.147$ |
| 3.31 | 8.67 | 100 | 2.73 | $y = 0.00461$ | 2.77 | $\tilde{t} = 0.232$ | 2.91 | $\delta_2 = 0.283$ |
| F–HCl | | −50 | 2.97 | $y = 0.00271$ | 3.57 | $\tilde{t} = 0.107$ | 3.16 | $\delta_1 = 0.234$ |
| 3.12 | 0.538 | 25 | 2.97 | $y = 0.00270$ | 2.92 | $\tilde{z} = -0.0861$ | 2.90 | $\delta_1 = 0.0698$ |
| 3.18 | 14.0 | 100 | 2.97 | $y = 0.00269$ | 3.00 | $\tilde{t} = 0.175$ | 3.22 | $\delta_2 = 0.244$ |
| F–HBr | | −50 | 3.16 | $y = 0.00169$ | 3.76 | $\tilde{t} = 0.0938$ | 3.35 | $\delta_1 = 0.179$ |
| 3.29 | 0.538 | 25 | 3.16 | $y = 0.00169$ | 3.09 | $\tilde{z} = -0.0777$ | 3.37 | $\delta_2 = 0.0518$ |
| 3.00 | 28.7 | 100 | 3.16 | $y = 0.00168$ | 3.19 | $\tilde{t} = 0.140$ | 3.38 | $\delta_2 = 0.206$ |
| F–Kr | | −50 | 2.99 | $y = 0.00245$ | 3.49 | $\tilde{t} = 0.133$ | 3.15 | $\delta_1 = 0.247$ |
| 3.10 | 0.631 | 25 | 2.99 | $y = 0.00244$ | 2.93 | $\tilde{z} = -0.106$ | 3.16 | $\delta_2 = 0.0690$ |
| 2.84 | 34.6 | 100 | 2.99 | $y = 0.00243$ | 3.01 | $\tilde{t} = 0.178$ | 3.17 | $\delta_2 = 0.280$ |
| F–$CH_4$ | | −50 | 2.98 | $y = 0.00457$ | 3.50 | $\tilde{t} = 0.176$ | 3.16 | $\delta_1 = 0.440$ |
| 3.11 | 0.632 | 25 | 2.98 | $y = 0.00454$ | 2.94 | $\tilde{z} = -0.142$ | 3.18 | $\delta_2 = 0.126$ |
| 2.75 | 36.7 | 100 | 2.98 | $y = 0.00452$ | 3.03 | $\tilde{t} = 0.242$ | 3.18 | $\delta_2 = 0.502$ |
| F–HI | | −50 | 3.46 | $y = 0.000829$ | 4.20 | $\tilde{t} = 0.0657$ | 3.72 | $\delta_1 = 0.118$ |
| 3.63 | 0.465 | 25 | 3.46 | $y = 0.000828$ | 3.40 | $\tilde{z} = -0.0559$ | 3.67 | $\delta_2 = 0.0424$ |
| 2.95 | 78.5 | 100 | 3.46 | $y = 0.000827$ | 3.49 | $\tilde{t} = 0.0940$ | 3.72 | $\delta_2 = 0.149$ |
| F–Xe | | −50 | 3.13 | $y = 0.00317$ | 3.58 | $\tilde{t} = 0.150$ | 3.27 | $\delta_1 = 0.272$ |
| 3.23 | 0.674 | 25 | 3.13 | $y = 0.00316$ | 3.06 | $\tilde{z} = -0.117$ | 3.31 | $\delta_2 = 0.0666$ |
| 2.30 | 147 | 100 | 3.13 | $y = 0.00314$ | 3.15 | $\tilde{t} = 0.208$ | 3.30 | $\delta_2 = 0.292$ |

In the series O–$^1S$, the potential well depths of the states $V_{20}$ and $V_{21}$ increase in the same order. The only exception is that the potential well depth of the state $V_{20}$ for the system O–$CH_4$ is smaller than that for the system O–Kr, see Table 4.

As an example, Figs. 4–7 show the curves $x(R)$, $y(R)$, $\tilde{z}(R)$ and $\tilde{t}(R)$ for the systems F–$CH_4$ and Cl–He at $E = 25$ meV, O–Ar ($\Omega = 0$) at $E = 100$ meV, and O–Xe ($\Omega = 1$) at $E = -50$ meV.

In each of the three series F–$^1S$, Cl–$^1S$, and O–$^1S$, the maximum position $R_p$ of the absolute value $|p(R)|$ of the nonadiabatic coupling matrix element increases

**Table 3.** Some characteristic features of the first-order post-adiabatic potentials and couplings for the Cl–$^1S$ systems. For the notations, see the text. The quantities $R_0$ and $\varepsilon$ refer to $u_2 = V_{3/2,1/2}$

| System | | $E$ (meV) | $R_{x,y}$ (Å) | $x$ or $y$ (Å$^{-1}$) | $R_{\tilde{z},\tilde{t}}$ (Å) | $\tilde{z}$ or $\tilde{t}$ (Å$^{-1}$) | $R_*$ (Å) | $\delta_1$ or $\delta_2$ (meV) |
|---|---|---|---|---|---|---|---|---|
| $R_p$ (Å)<br>$R_0$ (Å) | $\lvert p\rvert$ (Å$^{-1}$)<br>$\varepsilon$ (meV) | | | | | | | |
| Cl–He | | −50 | 1.84 | $y = 0.0340$ | 1.00 | $\tilde{t} = -1.64$ | 1.77 | $\delta_1 = 3.68$ |
| 1.89 | 0.524 | 25 | 1.83 | $y = 0.0338$ | 1.00 | $\tilde{t} = -1.64$ | 1.76 | $\delta_1 = 3.48$ |
| 3.45 | 2.85 | 100 | 1.83 | $y = 0.0337$ | 1.00 | $\tilde{t} = -1.63$ | 1.74 | $\delta_1 = 3.28$ |
| Cl–Ne | | −50 | 2.37 | $y = 0.00303$ | 2.64 | $\tilde{t} = 0.145$ | 2.37 | $\delta_1 = 0.374$ |
| 2.45 | 0.538 | 25 | 2.37 | $y = 0.00303$ | 2.56 | $\tilde{t} = 0.145$ | 2.33 | $\delta_1 = 0.310$ |
| 3.49 | 6.04 | 100 | 2.37 | $y = 0.00303$ | 2.51 | $\tilde{t} = 0.159$ | 2.29 | $\delta_1 = 0.255$ |
| Cl–$D_2$ | | −50 | 2.64 | $y = 0.00625$ | 3.02 | $\tilde{t} = 0.142$ | 2.71 | $\delta_1 = 0.857$ |
| 2.74 | 0.539 | 25 | 2.64 | $y = 0.00623$ | 2.85 | $\tilde{t} = 0.121$ | 2.64 | $\delta_1 = 0.604$ |
| 3.48 | 8.31 | 100 | 2.64 | $y = 0.00621$ | 2.75 | $\tilde{t} = 0.157$ | 2.55 | $\delta_1 = 0.410$ |
| Cl–Ar | | −50 | 2.85 | $y = 0.00176$ | 3.12 | $\tilde{t} = 0.0982$ | 2.86 | $\delta_1 = 0.219$ |
| 2.92 | 0.544 | 25 | 2.85 | $y = 0.00176$ | 3.03 | $\tilde{t} = 0.0974$ | 2.81 | $\delta_1 = 0.173$ |
| 3.78 | 14.9 | 100 | 2.85 | $y = 0.00175$ | 2.97 | $\tilde{t} = 0.111$ | 2.76 | $\delta_1 = 0.135$ |
| Cl–Kr | | −50 | 3.12 | $y = 0.000822$ | 3.51 | $\tilde{t} = 0.0432$ | 3.19 | $\delta_1 = 0.108$ |
| 3.22 | 0.544 | 25 | 3.12 | $y = 0.000822$ | 3.02 | $\tilde{z} = -0.0421$ | 3.11 | $\delta_1 = 0.0710$ |
| 3.75 | 22.0 | 100 | 3.12 | $y = 0.000821$ | 3.21 | $\tilde{t} = 0.0573$ | 3.00 | $\delta_1 = 0.0448$ |
| Cl–$CH_4$ | | −50 | 3.21 | $y = 0.00136$ | 3.13 | $\tilde{z} = -0.0633$ | 3.34 | $\delta_1 = 0.197$ |
| 3.33 | 0.544 | 25 | 3.21 | $y = 0.00135$ | 3.13 | $\tilde{z} = -0.0632$ | 3.25 | $\delta_1 = 0.107$ |
| 3.44 | 27.5 | 100 | 3.21 | $y = 0.00135$ | 3.13 | $\tilde{z} = -0.0632$ | 3.45 | $\delta_2 = 0.120$ |
| Cl–Xe | | −50 | 3.38 | $y = 0.000697$ | 3.31 | $\tilde{z} = -0.0493$ | 3.51 | $\delta_1 = 0.0942$ |
| 3.49 | 0.608 | 25 | 3.38 | $y = 0.000696$ | 3.31 | $\tilde{z} = -0.0493$ | 3.43 | $\delta_1 = 0.0481$ |
| 3.23 | 35.4 | 100 | 3.38 | $y = 0.000696$ | 3.31 | $\tilde{z} = -0.0493$ | 3.59 | $\delta_2 = 0.0637$ |

rapidly as one goes from He to Xe in the order shown by the sequence (28), the maximum value of the function $|p(R)|$ itself changing only very slightly (for the interactions O–$^1S$, this holds for both the two-state subsystems with $\Omega = 0$ and $\Omega = 1$). On the other hand, as one goes from $^1S$ = He to $^1S$ = Xe, the minimum location (equilibrium distance) of the ground state varies in a considerably smaller range (for the O–$^1S$ systems, the equilibrium distance increases, while for the F–$^1S$ and Cl–$^1S$ systems, it changes in an irregular way). Consequently, as one goes from $^1S$ = He to $^1S$ = Xe in the order given by the sequence (28), the interaction $^{2,3}P$–$^1S$ is becoming of more and more prominent molecular character [33] (it corresponds to the Hund case *c* for $^1S$ = He and to the Hund case *a* for $^1S$ = Xe).

The behavior of the first-order post-adiabatic potentials $u_1^{(1)}$, $u_2^{(1)}$ and coupling matrices $\Pi_1$ (to be more precise, the functions $x$, $y$, $\tilde{z}$, $\tilde{t}$) for the systems in question suggests the following remarks (see Tables 2–5).

(1) The functions $x$, $y$, $\tilde{z}$, $\tilde{t}$ describing the first-order post-adiabatic coupling $\Pi_1$ and the differences $\delta_1 = u_1 - u_1^{(1)}$, $\delta_2 = u_2 - u_2^{(1)}$ of the adiabatic and first-order post-adiabatic potentials attain their absolute value maxima near the maximum point of the usual nonadiabatic coupling matrix element $p$. The reason is that the larger the nonadiabatic coupling $P$, the larger all the post-adiabatic couplings $\Pi_s$.

**Table 4.** Some characteristic features of the first-order post-adiabatic potentials and couplings for the O–$^1S$ systems corresponding to the states with $\Omega = 0$. For the notations, see the text. The quantities $R_0$ and $\varepsilon$ refer to $u_2 = V_{20}$

| System | | $E$ (meV) | $R_{x,y}$ (Å) | $x$ or $y$ (Å$^{-1}$) | $R_{\tilde{z},\tilde{t}}$ (Å) | $\tilde{z}$ or $\tilde{t}$ (Å$^{-1}$) | $R_*$ (Å) | $\delta_1$ or $\delta_2$ (meV) |
|---|---|---|---|---|---|---|---|---|
| $R_p$ (Å)<br>$R_0$ (Å) | $\lvert p_0 \rvert$ (Å$^{-1}$)<br>$\varepsilon$ (meV) | | | | | | | |
| O–He | | $-50$ | Potentials $u_1^{(1)}$, $u_2^{(1)}$ are complex for $2.46 \leqslant R$ (Å) $\leqslant 2.70$ | | | | | |
| 2.53 | 1.26 | 25 | 2.47 | $y = 0.445$ | 2.56 | $\tilde{t} = -2.11$ | 2.45 | $\delta_1 = 3.79$ |
| 3.40 | 1.62 | 100 | 2.43 | $y = 0.273$ | 2.44 | $\tilde{t} = -3.13$ | 2.59 | $\delta_2 = 8.05$ |
| O–Ne | | $-50$ | 2.58 | $y = 0.214$ | 2.76 | $\tilde{t} = -2.90$ | 2.60 | $\delta_1 = 4.60$ |
| 2.61 | 1.13 | 25 | 2.55 | $y = 0.162$ | 2.64 | $\tilde{t} = -1.56$ | 2.50 | $\delta_1 = 1.66$ |
| 3.39 | 3.53 | 100 | 2.53 | $y = 0.135$ | 2.54 | $\tilde{t} = -2.36$ | 2.70 | $\delta_2 = 2.48$ |
| O–D$_2$ | | $-50$ | 2.91 | $y = 2.02$ | 2.95 | $\tilde{t} = -19.8$ | 2.91 | $\delta_1 = 13.9$ |
| 2.88 | 1.06 | 25 | 2.80 | $y = 0.274$ | 2.88 | $\tilde{t} = -1.61$ | 2.74 | $\delta_1 = 2.50$ |
| 3.61 | 3.61 | 100 | 2.76 | $y = 0.195$ | 2.77 | $\tilde{t} = -2.67$ | 2.95 | $\delta_2 = 6.36$ |
| O–Ar | | $-50$ | 3.05 | $y = 0.0695$ | 3.32 | $\tilde{t} = -1.35$ | 3.13 | $\delta_1 = 2.33$ |
| 3.12 | 1.08 | 25 | 3.04 | $y = 0.0605$ | 3.10 | $\tilde{t} = -0.690$ | 2.95 | $\delta_1 = 0.441$ |
| 3.71 | 6.31 | 100 | 3.02 | $y = 0.0543$ | 3.02 | $\tilde{t} = -1.68$ | 3.18 | $\delta_2 = 2.29$ |
| O–Kr | | $-50$ | 3.27 | $y = 0.0411$ | 3.59 | $\tilde{t} = -0.947$ | 3.37 | $\delta_1 = 1.60$ |
| 3.36 | 1.03 | 25 | 3.26 | $y = 0.0374$ | 3.31 | $\tilde{t} = -0.514$ | 3.46 | $\delta_2 = 0.407$ |
| 3.86 | 7.31 | 100 | 3.25 | $y = 0.0346$ | 3.25 | $\tilde{t} = -1.41$ | 3.41 | $\delta_2 = 1.87$ |
| O–CH$_4$ | | $-50$ | 3.30 | $y = 0.0698$ | 3.60 | $\tilde{t} = -1.31$ | 3.40 | $\delta_1 = 2.72$ |
| 3.38 | 1.03 | 25 | 3.28 | $y = 0.0594$ | 3.33 | $\tilde{t} = -0.633$ | 3.47 | $\delta_2 = 0.697$ |
| 3.86 | 7.21 | 100 | 3.26 | $y = 0.0527$ | 3.26 | $\tilde{t} = -1.70$ | 3.43 | $\delta_2 = 3.05$ |
| O–Xe | | $-50$ | 3.51 | $y = 0.0305$ | 3.87 | $\tilde{t} = -0.773$ | 3.63 | $\delta_1 = 1.32$ |
| 3.61 | 1.00 | 25 | 3.51 | $y = 0.0282$ | 3.54 | $\tilde{t} = -0.451$ | 3.69 | $\delta_2 = 0.455$ |
| 4.00 | 9.25 | 100 | 3.50 | $y = 0.0264$ | 3.49 | $\tilde{t} = -1.32$ | 3.67 | $\delta_2 = 1.78$ |

(2) The elements $x$ and $y$ in all the cases turn out to be much smaller than $\tilde{z}$ and $\tilde{t}$ (as a rule, more than an order of magnitude). At the same time, the maximal values of the functions $|x|$ and $|y|$ do not differ considerably. The same is valid for the functions $|\tilde{z}|$ and $|\tilde{t}|$ as well, although the dimension correction given by Eqs. (26)–(27) is rather arbitrary. In all the cases, the maximum of $|y|$ is larger than that of $|x|$.

(3) As one goes along the series F–$^1S$ and Cl–$^1S$ from $^1S$ = He to $^1S$ = Xe in the order shown by the sequence (28), the first-order post-adiabatic coupling $\Pi_1$ weakens rapidly and the differences $\delta_1$ and $\delta_2$ decrease rapidly. Recall that the strength of the usual nonadiabatic coupling $P$ is almost the same for all the systems in each series. Starting from $^1S$ = Ar, the differences $\delta_1$ and $\delta_2$ become negligible, i.e., the first-order post-adiabatic potentials begin almost coinciding with the adiabatic potentials. The same trends in the behavior of $\Pi_1$, $\delta_1$, and $\delta_2$ are present for the O–$^1S$ interactions as well, but in a much less clear form.

(4) For the F–$^1S$ and Cl–$^1S$ systems, the first-order post-adiabatic potentials and coupling matrices exhibit almost no dependence on the total energy $E$, at least in the range $-50 \leqslant E \leqslant 100$ meV. For the O–$^1S$ systems, the potentials $u_1^{(1)}$, $u_2^{(1)}$ and matrices $\Pi_1$ strongly depend on $E$.

**Table 5.** Some characteristic features of the first-order post-adiabatic potentials and couplings for the O–$^1S$ systems corresponding to the states with $\Omega = 1$. For the notations, see the text. The quantities $R_0$ and $\varepsilon$ refer to $u_2 = V_{21}$

| System | | $E$ (meV) | $R_{x,y}$ (Å) | $x$ or $y$ (Å$^{-1}$) | $R_{\tilde{z},\tilde{t}}$ (Å) | $\tilde{z}$ or $\tilde{t}$ (Å$^{-1}$) | $R_*$ (Å) | $\delta_1$ or $\delta_2$ (meV) |
|---|---|---|---|---|---|---|---|---|
| $R_p$ (Å) | $\lvert p_1 \rvert$ (Å$^{-1}$) | | | | | | | |
| $R_0$ (Å) | $\varepsilon$ (meV) | | | | | | | |
| O–He | | −50 | 2.67 | $y = 0.486$ | 2.78 | $\tilde{t} = -7.16$ | 2.68 | $\delta_1 = 8.78$ |
| 2.64 | 0.893 | 25 | 2.55 | $y = 0.177$ | 2.62 | $\tilde{t} = -1.23$ | 2.46 | $\delta_1 = 1.15$ |
| 3.32 | 1.85 | 100 | 2.52 | $y = 0.132$ | 2.52 | $\tilde{t} = -2.63$ | 2.71 | $\delta_2 = 5.76$ |
| O–Ne | | −50 | 2.66 | $y = 0.0773$ | 2.98 | $\tilde{t} = -1.32$ | 2.73 | $\delta_1 = 2.00$ |
| 2.73 | 0.806 | 25 | 2.64 | $y = 0.0670$ | 2.71 | $\tilde{t} = -0.905$ | 2.52 | $\delta_1 = 0.530$ |
| 3.33 | 3.94 | 100 | 2.63 | $y = 0.0600$ | 2.63 | $\tilde{t} = -1.85$ | 2.82 | $\delta_2 = 1.89$ |
| O–D$_2$ | | −50 | 2.95 | $y = 0.164$ | 3.25 | $\tilde{t} = -2.31$ | 3.03 | $\delta_1 = 4.84$ |
| 3.00 | 0.756 | 25 | 2.89 | $y = 0.111$ | 2.95 | $\tilde{t} = -1.00$ | 3.14 | $\delta_2 = 1.03$ |
| 3.52 | 4.23 | 100 | 2.86 | $y = 0.0899$ | 2.86 | $\tilde{t} = -2.17$ | 3.08 | $\delta_2 = 4.53$ |
| O–Ar | | −50 | 3.15 | $y = 0.0298$ | 3.56 | $\tilde{t} = -0.793$ | 3.27 | $\delta_1 = 1.14$ |
| 3.24 | 0.775 | 25 | 3.13 | $y = 0.0274$ | 3.18 | $\tilde{t} = -0.520$ | 3.35 | $\delta_2 = 0.400$ |
| 3.61 | 7.25 | 100 | 3.12 | $y = 0.0256$ | 3.13 | $\tilde{t} = -1.40$ | 3.31 | $\delta_2 = 1.57$ |
| O–Kr | | −50 | 3.37 | $y = 0.0180$ | 3.85 | $\tilde{t} = -0.595$ | 3.52 | $\delta_1 = 0.806$ |
| 3.48 | 0.733 | 25 | 3.36 | $y = 0.0170$ | 3.40 | $\tilde{t} = -0.407$ | 3.58 | $\delta_2 = 0.344$ |
| 3.73 | 8.78 | 100 | 3.35 | $y = 0.0162$ | 3.36 | $\tilde{t} = -1.16$ | 3.56 | $\delta_2 = 1.25$ |
| O–CH$_4$ | | −50 | 3.39 | $y = 0.0297$ | 3.86 | $\tilde{t} = -0.801$ | 3.55 | $\delta_1 = 1.36$ |
| 3.50 | 0.732 | 25 | 3.38 | $y = 0.0270$ | 3.41 | $\tilde{t} = -0.506$ | 3.59 | $\delta_2 = 0.577$ |
| 3.71 | 8.81 | 100 | 3.37 | $y = 0.0249$ | 3.37 | $\tilde{t} = -1.42$ | 3.58 | $\delta_2 = 2.05$ |
| O–Xe | | −50 | 3.62 | $y = 0.0136$ | 4.13 | $\tilde{t} = -0.513$ | 3.79 | $\delta_1 = 0.682$ |
| 3.74 | 0.718 | 25 | 3.61 | $y = 0.0129$ | 3.63 | $\tilde{t} = -0.370$ | 3.82 | $\delta_2 = 0.351$ |
| 3.81 | 11.6 | 100 | 3.60 | $y = 0.0124$ | 3.61 | $\tilde{t} = -1.09$ | 3.81 | $\delta_2 = 1.18$ |

**Table 6.** The minimum location $\bar{R}_0$ and the potential well depth $\bar{\varepsilon}$ of the ground state $V_{22}(R)$ for the O–$^1S$ systems

| System | O–He | O–Ne | O–D$_2$ | O–Ar | O–Kr | O–CH$_4$ | O–Xe |
|---|---|---|---|---|---|---|---|
| $\bar{R}_0$ (Å) | 3.11 | 3.20 | 3.35 | 3.45 | 3.57 | 3.56 | 3.69 |
| $\bar{\varepsilon}$ (meV) | 2.97 | 5.43 | 6.49 | 10.4 | 13.1 | 13.4 | 17.3 |

(5) In general, the first-order post-adiabatic coupling $\Pi_1$ for the F–$^1S$ systems is *stronger* than that for the Cl–$^1S$ systems, and that for the O–$^1S$ systems (for both $\Omega = 0$ and $\Omega = 1$) is *much stronger* than that for F–$^1S$. Recall again that the strength of the usual nonadiabatic coupling $P$ depends slightly not only on the target molecule $^1S$, but also on the projectile atom $^{2,3}P$. The same law takes place for the differences $\delta_1$ and $\delta_2$ as well: in general they increase considerably as one passes from Cl to F and from F to O. The reason is that the strength of $\Pi_1$ is very sensitive to the difference $u_1 - u_2$ between the two adiabatic potentials of the two-state

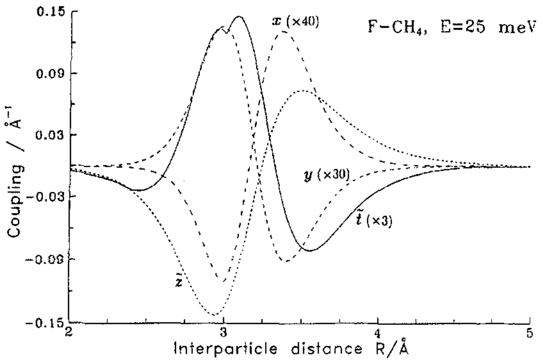

**Fig. 4.** The first-order post-adiabatic coupling curves for the F–CH$_4$ interaction at $E = 25$ meV. The fracture point on the curve $\tilde{t} = \tilde{t}(R)$ at $R = 3$ Å corresponds to sewing together two different analytical formulas representing the spherical component of the interaction [34]

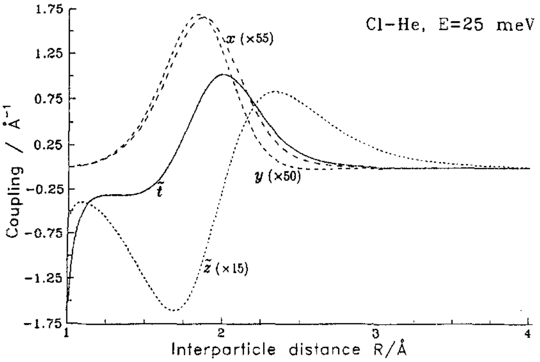

**Fig. 5.** The first-order post-adiabatic coupling curves for the Cl–He interaction at $E = 25$ meV

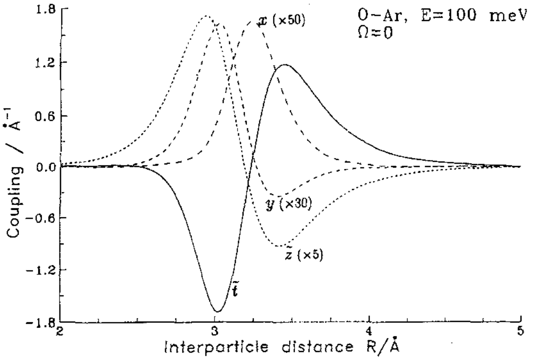

**Fig. 6.** The first-order post-adiabatic coupling curves (corresponding to the states with $\Omega = 0$) for the O–Ar interaction at $E = 100$ meV

subsystem in question: the larger this difference, the weaker the coupling $\Pi_1$. The difference $u_1 - u_2$ is mainly determined by the fine splitting of the energy levels of the projectile atom (and coincides with the splitting at $R = \infty$). The energy separation between the fine structure components of the projectile atom is equal to $E(^2P_{1/2}) - E(^2P_{3/2}) = 109.4$ meV for chlorine, $E(^2P_{1/2}) - E(^2P_{3/2}) = 50.1$ meV

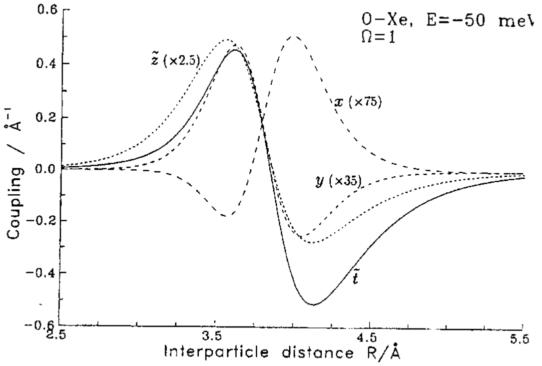

**Fig. 7.** The first-order post-adiabatic coupling curves (corresponding to the states with $\Omega = 1$) for the O–Xe interaction at $E = -50$ meV

for fluorine, and $E(^3P_0) - E(^3P_2) = 28.14\,\text{meV}$, $E(^3P_1) - E(^3P_2) = 19.62\,\text{meV}$ for oxygen [$E(^{2,3}P_j)$ denoting the energy of the corresponding term].

The ultimate purpose of the post-adiabatic representations is the reduction in the coupling between the potentials and, as a consequence, a more effective calculation of multichannel processes. The post-adiabatic approach makes therefore sense only for systems F–Ar, Kr, Xe, $CH_4$, HCl, HBr, HI and Cl–Ne, Ar, Kr, Xe, $D_2$, $CH_4$ where the first-order post-adiabatic coupling $\Pi_1$ does turn out to be *much smaller* than the initial nonadiabatic coupling $P$. On the other hand, one should expect that for the interaction of Br and I atoms with rare gas atoms and hydrogen, methane, and hydrogen halide molecules, the post-adiabatic scheme would lead to a coupling reduction even much more considerable than that for the Cl–$^1S$ systems.

## 8 Concluding remarks

The post-adiabatic representations have never been exploited yet in actual integration of multichannel Schrödinger equations. The main problem here is to work out an adequate technique to handle the more complicated structure of the post-adiabatic coupling matrices. This problem is interesting to tackle because for systems with a large separation between the adiabatic potentials (like Cl–$^1S$ in our examples) the first-order post-adiabatic representation seems to be more natural than the usual adiabatic one.

It would be also of interest to calculate the post-adiabatic potentials $u^{(s)}_{1,2}$ and couplings $\Pi_s$ of higher orders $s \geqslant 2$ for the systems F–$^1S$ and Cl–$^1S$. As we already pointed out in Sect. 4, no convergence criteria for the Klar–Fano procedure as $s \to \infty$ are known, and one is not aware even of conditions which would guarantee the inequalities $\eta_s < \eta_{s-1}$ for each $s \geqslant 1$ where $\eta_s$ are some quantities measuring the magnitude of the couplings $\Pi_s$. Moreover, even if the convergence does occur, its limit may be only approximate, i.e., the limit functions do not necessarily satisfy Eq. (15) exactly. If this is the case, there is a remainder of the interaction not taken into account.

Another interesting problem is to calculate the post-adiabatic potentials and couplings for systems with more than two states, although the two-state case is much more important for reasons explained at the beginning of Sect. 6. For systems with $N \geqslant 3$ states, even the simplest form of the coupling matrix $\Pi_1$ (expected to be achieved for $S_0 = S_0^*$) is still unknown, so the post-adiabatic treatment of such systems would be intriguing from the theoretical viewpoint.

*Acknowledgments.* This work is partially supported by the Italian Consiglio Nazionale delle Ricerche (Progetti Finalizzati Chimica Fine and Sistemi Informatici e Calcolo Parallelo). We are grateful to Professor U. Fano for sending us his preprint [25] prior to publication. Part of this work was performed at the H.C. Ørsted Institute in Copenhagen, and one of the authors (M.B.S.) acknowledges receiving a DANVIS scholarship from the Danish Research Academy. He is also partially supported by the International Fund "Cultural Initiative".

## Appendix. The regularity of the post-adiabatic representations at the turning points

What can be dangerous to the post-adiabatic scheme are the turning points $u_k^{(s)}(R) = E$ and the coalescence points $u_k^{(s)}(R) = u_l^{(s)}(R)$, $s \geqslant 1$, where the spectrum of the matrix $K_{s-1}(R)$ becomes multiple. At the turning and coalescence points of the post-adiabatic potentials of order $s$, the post-adiabatic coupling $\Pi_s = S_{s-1}^{-1}\, \mathrm{d}S_{s-1}/\mathrm{d}R$ of order $s$ and the post-adiabatic potentials $u_k^{(v)}$ and couplings $\Pi_v$ of all the orders $v \geqslant s+1$ are *a priori* not defined.

The coalescence points occur only for very low energies $E$ (much lower than the values of any physical significance) or very strong couplings $\Pi_{s-1}$. These points are therefore not of great interest for practical applications. On the other hand, the turning points are present just for the values of $E$ typical for the process in question, and are among the key objects determining the system dynamics in both the classical and quantum mechanical descriptions. If the matrix-valued function $S = S_{s-1}(R)$ did lose smoothness at the turning points of the post-adiabatic potentials of order $s$, the perspectives for applications of the post-adiabatic approach would be quite restrictive.

Fortunately, the function $S_{s-1}(R) = S_{s-1}^*(R)$ constructed according to the algorithm of Ref. [1] keeps its smoothness at the turning points $u_k^{(s)}(R) = E$. Hence, the post-adiabatic coupling $\Pi_s$ of order $s$ and all the subsequent post-adiabatic potentials $u_k^{(v)}$ and couplings $\Pi_v$, $v \geqslant s+1$, are well defined at these turning points. Since we did not pay adequate attention in Ref. [1] to this fact of fundamental importance for post-adiabatic analysis, we dwell upon it now. Note that for the systems O, F, Cl–$^1S$ considered in Sect. 7, we observed no singularities of $\Pi_1$ at the turning points of $u_1^{(1)}$ and $u_2^{(1)}$.

Let $R_0$ be a turning point of the post-adiabatic potential $u_1^{(s)}(R)$ corresponding to the total energy $E$, i.e., $u_1^{(s)}(R_0) = E$. At $R = R_0$ the matrix

$$K_{s-1} = \begin{pmatrix} A & B \\ C & -A^{\mathrm{t}} \end{pmatrix}$$

(where $A$, $B$, $C$ are $N \times N$ matrices, $B$ and $C$ being symmetric) possesses the zero eigenvalue of multiplicity two (we will sometimes drop the index $s-1$). If $\pm\lambda_1$, $\pm\lambda_2$, … , $\pm\lambda_N$ are all the eigenvalues of the matrix $K_{s-1}$ then $u_k^{(s)} = \lambda_k^2 + E$ and $\lambda_1(R_0) = 0$. For a generic turning point $R_0$ the following holds.

(1) The matrix $K_{s-1}(R)$ and all the potentials $u_k^{(s)}(R)$ depend smoothly on the "slow" coordinate $R$ near $R_0$.

(2) The potentials $u_1^{(s)}(R), u_2^{(s)}(R), \ldots, u_N^{(s)}(R)$ are pairwise distinct at any $R$ close to $R_0$.

(3) $\mathrm{d}u_1^{(s)}(R_0)/\mathrm{d}R \neq 0$ (in fact, this condition is not essential for the smoothness of $S^*_{s-1}(R)$ at $R_0$).

(4) The matrix $B(R)$ is not singular at all $R$ close to $R_0$.

Turning points of more complicated structures for which these assumptions fail occur for some isolated values of the total energy $E$ only and are therefore of little importance in practical calculations.

Note that the functions $\lambda_k(R)$ for $k \neq 1$ and the function $\lambda_1^2(R)$ are smooth whereas, according to condition (3) above, the function $\lambda_1(R) = [u_1^{(s)}(R) - E]^{1/2}$ has a root singularity at point $R = R_0$.

According to Ref. [1], at all $R$ close to $R_0$ (with the possible exception of the turning point $R = R_0$ itself), each of the $N \times N$ matrices

$$T_k^{\pm} = C + (A^t \pm \lambda_k I)B^{-1}(A \mp \lambda_k I), \quad k = 1, 2, \dots, N,$$

is of rank $N - 1$. Suppose in addition that

(5) the 0-eigensubspace of each of these matrices $T_k^{\pm}$ does not lie in the $k$th coordinate hyperplane

$$\{\text{the } k\text{th coordinate is equal to zero}\}.$$

Under these assumptions, the algorithm for the choice of the matrix $S = S_{s-1}(R)$ at $R \neq R_0$ proposed in Ref. [1] consists of the following. Denote the 0-eigenvector of the matrix $T_k^{\pm}$ whose $k$th coordinate is equal to 1 by $f_{k,*}^{\pm}$. Consider the $2N$-dimensional vector

$$g_k^{\pm} = \begin{pmatrix} f_{k,*}^{\pm} \\ B^{-1}(\pm\lambda_k I - A) f_{k,*}^{\pm} \end{pmatrix}.$$

According to Ref. [1], the vectors $g_k^{\pm}$ are $(\pm\lambda_k)$-eigenvectors of the matrix

$$\begin{pmatrix} 0 & I \\ U_s - EI & 0 \end{pmatrix}.$$

Now recall that the skew-scalar product of vectors $a = (a_1, \dots, a_{2N})$ and $b = (b_1, \dots, b_{2N})$ is defined as

$$\langle a, b \rangle = \sum_{l=1}^{N} (a_l b_{N+l} - a_{N+l} b_l).$$

Let the skew-scalar product of the vectors $g_k^+$ and $g_k^-$ be equal to $-2\lambda_k \zeta_k$ where $\zeta_k \neq 0$ is a certain number. Set

$$v_k = \frac{f_{k,*}^{+} + f_{k,*}^{-}}{2\zeta_k^{1/2}}, \qquad w_k = \frac{f_{k,*}^{+} - f_{k,*}^{-}}{2\lambda_k \zeta_k^{1/2}}.$$

Denote by $V$ and $W$ the $N \times N$ matrices with columns $v_1, v_2, \dots, v_N$ and $w_1, w_2, \dots, w_N$, respectively, and define the matrices $X$, $Y$, and the desired matrix $S^*_{s-1}$ in the following way:

$$X = B^{-1}[W(U_s - EI) - AV], \qquad Y = B^{-1}(V - AW), \qquad S^*_{s-1} = \begin{pmatrix} V & W \\ X & Y \end{pmatrix}.$$

We wish to prove that the matrix-valued function $S^*_{s-1}(R)$ can be smoothly continued into the point $R = R_0$. In fact, it suffices to verify that the vectors $v_1$ and $w_1$ depend on $R$ smoothly in a neighborhood of $R_0$. The matrix $C + A^t B^{-1} A$ is singular at the point $R = R_0$. Impose the additional genericity condition:

(6) The $N \times N$ matrix $C + A^{t}B^{-1}A$ is of rank $N - 1$ at $R = R_0$, and its 0-eigensubspace does not lie in the first coordinate hyperplane.

Treating $\lambda \in \boldsymbol{C}$ and $R$ as independent variables, consider the $N \times N$ matrix

$$C + (A^{t} + \lambda I)B^{-1}(A - \lambda I).$$

For $R$ close to $R_0$ and $\lambda$ close to 0, this matrix possesses the eigenvalue $\Lambda(R, \lambda)$ which smoothly depends on $R$, holomorphically depends on $\lambda$, and vanishes at $R = R_0$, $\lambda = 0$. Note that $\Lambda(R, \pm\lambda_1(R)) \equiv 0$. Let $F(R, \lambda)$ be the corresponding eigenvector whose first coordinate is equal to 1. Note that $F(R, \pm\lambda_1(R)) = f^{\pm}_{1,*}(R)$. The vector $F(R, \lambda)$ smoothly depends on $R$ and holomorphically on $\lambda$.

The vector-valued functions

$$F(R, \lambda) + F(R, -\lambda) = F_1(R, \lambda^2), \qquad \frac{F(R, \lambda) - F(R, -\lambda)}{\lambda} = F_2(R, \lambda^2)$$

even in $\lambda$ are smooth in their first argument $R$ and holomorphic in the second one $\lambda^2$.

Now consider the skew-scalar product $Z(R, \lambda)$ of the $2N$-dimensional vectors

$$\begin{pmatrix} F(R, \lambda) \\ B^{-1}(\lambda I - A)F(R, \lambda) \end{pmatrix} \text{ and } \begin{pmatrix} F(R, -\lambda) \\ -B^{-1}(\lambda I + A)F(R, -\lambda) \end{pmatrix}.$$

The function $Z(R, \lambda)$ is smooth in $R$ and holomorphic in $\lambda$. Moreover, $Z(R, \lambda)$ is odd in $\lambda$ and can therefore be represented in the form

$$Z(R, \lambda) = \lambda Z_0(R, \lambda^2),$$

where the function $Z_0$ is smooth in its first argument $R$ and holomorphic in the second one $\lambda^2$. Suppose that

(7) $Z_0(R_0, 0) \neq 0$.

This condition is also a nondegeneracy assumption, i.e., it fails only for some isolated exceptional values of the total energy $E$. To verify this, it is sufficient to consider the simplest case where $C$ is a diagonal matrix, $B \equiv I$, and $A \equiv 0$. In this case, $Z(R, \lambda) = -2\lambda$ and $Z_0(R, \lambda) \equiv -2$.

Now one has

$$v_1(R) = \frac{F_1(R, \lambda_1^2(R))}{[-2Z_0(R, \lambda_1^2(R))]^{1/2}}, \qquad w_1(R) = \frac{F_2(R, \lambda_1^2(R))}{[-2Z_0(R, \lambda_1^2(R))]^{1/2}},$$

The vector-valued functions $v_1(R)$ and $w_1(R)$ are smooth at the point $R = R_0$ because the function $\lambda_1^2(R)$ is smooth.

## References

1. Aquilanti V, Cavalli S, Sevryuk MB (1994) J Math Phys 35:536
2. Born M, Oppenheimer R (1927) Ann Phys 84:457
3. Smith FT (1969) Phys Rev 179:111
4. Garrett BC, Truhlar DG (1981) In: Theoretical chemistry: advances and perspectives, Vol 6A. Academic Press, New York, p 215; Garrett BC, Truhlar DC, Melius CF (1983) In: Hinze J (ed) Energy storage and redistribution in molecules. Plenum, New York, p 375

5. Tully JC (1976) In: Miller WH (ed) Dynamics of molecular collisions, Part B (Modern theoretical chemistry, Vol 2). Plenum, New York, p 217
6. Lichten W (1963) Phys Rev 131:229
7. O'Malley TF (1971) Adv At Mol Phys 7:223
8. Baer M (1975) Chem Phys Lett 35:112
9. Baer M, Drolshagen G, Toennies JP (1980) J Chem Phys 73:1690; Baer M (1985) In: Baer M (Ed) Theory of chemical reaction dynamics, Vol 2. CRC Press, Boca Raton, FL, p 219; Baer M, Nakamura H (1987) J Chem Phys 87:4651
10. Bunker DL (1971) Methods Comput Phys 10:287
11. Porter RN, Raff LM (1976) In: Miller WH (ed) Dynamics of molecular collisions, Part B (Modern theoretical chemistry, Vol 2). Plenum, New York, p 1
12. Billing GD (1984) Comput Phys Rep 1:237
13. Billing GD (1991) Trends Chem Phys 1:133; (1993) In: Cerjan C (ed) Numerical grid methods and their application to Schrödinger's equation (NATO ASI Series C, Vol 412). Kluwer, Dordrecht, p 121
14. Muckerman JT, Gilbert RD, Billing GD (1988) J Chem Phys 88:4779; Billing GD, Muckerman JT (1989) ibid. 91:6830; Markovič N, Billing GD, Muckerman JT (1990) Chem Phys Lett 172:509
15. Markovič N, Billing GD (1992) J Chem Phys 97:8201; (1993) Chem Phys 173:385
16. Aquilanti V, Grossi G, Laganà A (1982) Chem Phys Lett 93:174; Aquilanti V, Cavalli S, Laganà A (1982) ibid 93:179; Aquilanti V, Cavalli S, Grossi G (1987) ibid 133:531; Aquilanti V, Cavalli S (1987) ibid 133:538; Aquilanti V, Cavalli S, Grossi G (1989) Theor Chim Acta 75:33
17. Child MS (1976) In: Miller WH (ed) Dynamics of molecular collisions, Part B (Modern theoretical chemistry, Vol 2). Plenum, New York, p 171; Child MS (1991) Semiclassical mechanics with molecular applications. Clarendon, Oxford
18. Aquilanti V, Cavalli S, Grossi G (1993) In: Bowman JM (ed) Advances in molecular vibrations and collision dynamics, Vol 2A. JAI Press, p 147; Aquilanti V, Cavalli S, Sevryuk MB (1991) J Phys A 24:4475; Aquilanti V, Cavalli S, Sevryuk MB (1993) J Math Phys 34:3351
19. Chan S-K, Light JC, Lin J-L (1968) J Chem Phys 49:86
20. Wu S-F, Levine RD (1971) Mol Phys 22:881; Wu S-F, Johnson BR, Levine RD (1973) ibid. 25:609; 25:839
21. Mrugała F (1993) Intern Rev Phys Chem 12:1
22. Klar H, Fano U (1976) Phys Rev Lett 37:1132
23. Klar H (1977) Phys Rev A 15:1452
24. Klar H, Klar M (1978) Phys Rev A 17:1007
25. Bohn JL, Fano U (1993) preprint
26. Reznikov AI, Umanskiĭ SYa (1991) Sov J Chem Phys 8:2193
27. Fano U (1981) Phys Rev A 24:2402
28. Johnson BR (1980) J Chem Phys 73:5051; (1983) 79:1906; (1983) 79:1916
29. Aquilanti V, Cavalli S (1986) J Chem Phys 85:1355; Aquilanti V, Cavalli S, Grossi G (1986) ibid. 85:1362; Aquilanti V, Cavalli S (1987) Chem Phys Lett 141:309; Aquilanti V, Laganà A, Levine RD (1989) ibid. 158:87; Aquilanti V, Cavalli S, Grossi G, Pellizzari V, Rosi M, Sgamellotti A, Tarantelli F (1989) ibid. 162:179; Aquilanti V, Cavalli S, Grossi G, Anderson RW (1990) J Chem Soc Faraday Trans 86:1681; Aquilanti V, Cavalli S, Grossi G (1991) Theor Chim Acta 79:283; Aquilanti V, Cavalli S (1992) Few Body Systems Suppl 6:573; Aquilanti V, Cavalli S, Monnerville M (1993) In: Cerjan CC (ed) Numerical grid methods and their application to Schrödinger's equation. Kluwer Academic Publishers, p 25
30. Fock V (1958) K Nor Vidensk Selsk Forh 31:138
31. Leforestier C, Wyatt RE (1983) J Chem Phys 78:2334; Kosloff R, Kosloff D (1986) J Comput Phys 63:363; Neuhauser D, Baer M (1989) J Chem Phys 90:4351; Baer M, Neuhauser D, Oreg Y (1990) J Chem Soc Faraday Trans 86:1721; Child MS (1991) Mol Phys 72:89; Last I, Neuhauser D, Baer M (1992) J Chem Phys 96:2017; Baer M, Nakamura H (1992) ibid. 96:6565
32. Last I, Baram A, Baer M (1992) Chem Phys Lett 195:435; Baram A, Last I, Baer M (1993) ibid. 212:649; (1993) 215:416; Szichman H, Last I, Baram A, Baer M (1993) J Phys Chem 97:6436; Last I, Baram A, Szichman H, Baer M (1993) ibid. 97:7040
33. Aquilanti V, Liuti G, Pirani F, Vecchiocattivi F (1989) J Chem Soc Faraday Trans 2 85:955

34. Becker CH, Casavecchia P, Lee YT, Olson RE, Lester WA Jr (1979) J Chem Phys 70:5477; Aquilanti V, Luzzatti E, Pirani F, Volpi GG (1982) Chem Phys Lett 90:382; (1988) J Chem Phys 89:6165; Aquilanti V, Candori R, Cappelletti D, Pirani F (1990) In: Capitelli M, Bardsley JN (eds) Nonequilibrium processes in partially ionized gases (NATO ASI Series B, Vol 220). Plenum, New York, p 383; Aquilanti V, Candori R, Cappelletti D, Luzzatti E, Pirani F (1990) Chem Phys 145:293
35. Aquilanti V, Cappelletti D, Lorent V, Luzzatti E, Pirani F (1992) Chem Phys Lett 192:153; (1993) J Phys Chem 97:2063; Aquilanti V, Cappelletti D, Pirani F (1993) J Chem Soc Faraday Trans 89:1467
36. Aquilanti V, Cappelletti D, Pirani F, Rusin LYu, Sevryuk MB, Toennies JP (1991) J Phys Chem 95:8248
37. Aquilanti V, Luzzatti E, Pirani F, Volpi GG (1980) J Chem Phys 73:1181; Aquilanti V, Candori R, Luzzatti E, Pirani F, Volpi GG (1986) ibid. 85:5377; Aquilanti V, Candori R, Pirani F (1988) ibid. 89:6157; Aquilanti V, Candori R, Liuti G, Pirani F (1988) In: Whitehead JC (ed) Selectivity in chemical reactions (NATO ASI Series C, Vol 245). Kluwer, New York, p 179; Aquilanti V, Candori R, Mariani L, Pirani F, Liuti G (1989) J Phys Chem 93:130
38. Aquilanti V, Vecchiocattivi F (1989) Chem Phys Lett 156:109